AD-784 991

HIGH ENERGY LASER WINDOWS

R. W. Rice

Naval Research Laboratory

Prepared for:

Advanced Research Projects Agency

30 June 1974

High Energy Laser Windows

Semi-Annual Report No. 4
For period ending 30 June 1974

Sponsored by
Advanced Research Projects Agency
ARPA Order 2051

NAVAL RESEARCH LABORATORY
Washington, D.C. 20375

ARPA Order
2031

Program Code
3D10

Principal Investigator:
R. W. Rice
(202)767-2131

Contractor:
U. S. Naval Research Laboratory

Effective Date of Contract:
1 July 1973

Contract Expiration Date:
30 June 1974

Amount of Contract:
$225K

Forward

This semi-annual technical report summarizes work performed by personnel of the U. S. Naval Research Laboratory, Washington, D.C. 20375, under ARPA Order 2C31. The program was coordinated by Mr. R. W. Rice and Dr. P. F. Becher of NRL, and monitored by Dr. C. M. Stickley of ARPA. The report covers the period 1 January 1974 through 30 June 1974. The list of publications and presentations at the beginning of the report illustrate several of the major results of this program. The material contained in the Appendix was not supported by ARPA but is included since it should be of general interest to those concerned with laser windows.

Publications and Presentations

1. Davisson, J. W. (1974), "Surface Finishing of Alkali Halides," J. Mater. Sci., accepted for publication.

2. Hass, M., Davisson, J. W., Klein, P. H. and Boyer, L. L. (1974), "Infrared Absorption in Low Loss KCl Single Crystals Near 10.6μm," J. Appl. Phys., accepted for publication.

3. Boyer, L. L. and Rosenstock, H. B. (1974), "Multiphonon Absorption in Alkali Halides," Amer. Phys. Soc., Salt Lake City, Utah, June.

4. Becher, P. F., Rice, R. W., Klein, P. H., and Freiman, S. W. (1974), "Forging Behavior of KCl and Resultant Strengthening," Symp. on Deformation of Ceramic Materials, Pennsylvania State Univ., July; to be published in Symposium Proc., Plenum Press, New York.

5. Freiman, S. W., Becher, P. F. and Klein, P. H. (1974), "Crack Propagation in KCl," submitted to Phil. Mag.

TABLE OF CONTENTS

INTRODUCTION AND SUMMARY

Progress has continued toward our goals of understanding and diminishing absorption and increasing mechanical strength and toughness of alkali halides for laser window use. Work again has centered on KCl as both a viable candidate and a model for other halides.

During this reporting period, growth of pure and alloyed KCl of very low total absorption ($\beta<3\times10^{-4}cm^{-1}$) has continued with crystals also being supplied to several other organizations. Both vacuum UV and IR emittance spectra show absorption bands in pure KCl which increase with atmospheric exposure and may have a common origin as a surface phenomenon. The UV band is due probably to an oxygen species other than OH. The IR emittance studies demonstrate that the 9.5μm band, which can contribute to 10.6μm absorption, can be eliminated by heating in vacuum; this observation may be useful in coating operations.

To consolidate our understanding of multiphonon absorption, an extensive theoretical analysis of its frequency and temperature-dependence has been made and was consistent with existing data. It also has been used to predict behavior in crystals where data are not now available, and thus provides a valuable guide for work concerning new 10.6μm, as well as future 3.8μm, materials.

Forging studies have shown that the increased microstructural stability in KCl-$SrCl_2$ alloys allows forging at higher temperatures (up to 320°C), which

greatly reduces birefringence while maintaining reasonable yield strength (4000-5000 psi). Laser testing (10.6μm, 18 KW/cm^2, 6 mm dia., top hat beam) demonstrated that the birefringence enhances laser-induced window deformation, while yield strengths >3000 psi eliminated it. The fracture toughness of pure or alloyed forgings was shown to be uniformly high. On the other hand, the toughness of single crystals may increase with the yield stress (e.g., due to alloying or irradiation) but was dependent on strain rate, yield stress, and dislocation density. Experimental observations supported a fracture mechanism in KCl involving competition between dislocation processes of crack blunting and crack growth.

In addition to the above work, several results from associated studies are included because of their pertinence to the laser window programs. A "second generation" laser calorimetric technique has been devised for SiO_2 which, for the first time, separates surface and bulk absorption in a single measurement. Vacuum UV studies of NaF noted no change in absorption with air exposure in contrast to changes with more deliquescent KCl. Chemical polishing of short wavelength materials such as NaF, CaF_2, and BaF_2, though more difficult, showed promise. Fracture studies of ZnSe and As_2S_3 demonstrated that slow crack growth occurs, making their strengths stress history and environment sensitive. While surface flaws (especially corner flaws) were shown to dominate failure of ZnSe, results also indicated that internal flaws may have to be considered.

Future 10.6μm work would entail several changes. A further increase in preparation and characterization of low-loss KCl for other investigators is expected. Forging studies to further optimize the balance between

high strength and minimum birefringence will continue. Mechanical studies of KCl should be substantially completed next year, and will be coupled in part to increased laser testing. Substantial effort would be initiated in developing "second generation halides" such as KBr for absorption lower than KCl. The theoretical work should be completed to guide in the selection and growth of such materials. Adaptation of "second generation calorimetry," along with continued use of emittance studies, would be carried out to provide the characterization necessary for both new 10.6 and 3.8μm materials.

CHARACTERIZATION OF STRONTIUM-DOPED KCl FORGINGS

P.F.Becher, R.W.Rice, and M.Krulfeld
Naval Research Laboratory
Washington, D.C. 20375

1. INTRODUCTION

Recent studies have concentrated on the effect of forging at high temperatures to reduce the residual birefringence in, and optimize the strength of, strontium-doped KCl. Previous studies of KCl showed that minimal forging strains (>20%) are required to produce a polycrystalline-like microstructure (Becher et al, 1973). Above 60% forging, exaggerated grain growth is enhanced by residual strains (Becher et al, 1973, and Bernal et al, 1973). Forging temperatures in the range of 125° to 200°C do not significantly alter percent forging reduction-microstructure behavior, nor does the rate of deformation, though both should influence residual strain. Analysis of forging deformation behavior and resultant microstructures indicates that in KCl, the polycrystalline-like microstructure results from polygonization processes, and that the exaggerated grain growth above 60% reductions results from recrystallization (Becher et al, 1974b). Recovery and polygonization appear to occur so readily in KCl that recrystallization occurs only at high deformation strains, comparable to the behavior of Ag and Cu (Mecking and Kirch, 1971).

Previous studies have indicated that post-forging annealing can bring about recovery in forgings and reduce residual strain (Becher et al, 1973 and 1974a; Bernal et al, 1973; Kulin et al, 1974). However, pure

KCl forged at ≦ 200°C generally contains inhomogeneous birefringence banding and can be subject to grain growth during recovery anneal. Forging temperatures > 200°C are possible as alloying results in greater microstructural stability (e.g., slower grain growth, Becher et al, 1974a) than that in pure KCl. In the present studies, the effects of higher forging temperatures on (1) the reduction of birefringence, and (2) reduction in strength were studied in strontium-doped KCl.

2. RESULTS AND DISCUSSION

Alloyed (≦ 1500 ppma Sr^{+2} added to melt) forgings having grain sizes in the range of ≦ 15μm were produced at 60 to 70% height reductions in the temperature range of 200° to 340°C using Cu constraining rings to minimize cracking (Anderson et al, 1973, and Becher et al, 1974a). The birefringence in these bodies decreased with increasing forging temperature such that above 250°C, the strong birefringence bands normally observed are eliminated, Figure 1. Thus, locally high residual strains appear to be fully recovered by forging at 300°C, giving a forging which has lower and more homogeneous birefringence and lower residual strain (Figure 1). The temperature to relieve birefringence inhomogeneities is not altered significantly by strontium content, but one 1500 ppma Sr^{+2}-doped forging at 320°C exhibit only very faint 10μm sub-grains within large grain regions. At or below 320°C, forgings of strontium-doped crystals (≦ 1500 ppma) gave distinct fine-grained (< 10μm) microstructures. Thus, forging temperatures to reduce residual birefringence appears to be limited to 250° to 300°C to obtain distinct polycrystalline microstructures for alloys of ≦ 1500 ppma strontium.

It was noted earlier that post-forging anneals can result in loss of strength of KCl forgings (Becher et al, 1974a); thus the effect of forging temperature on strength was considered next. The yield strength of the alloyed forgings decreases with increase in forging temperature, Figure 2, from ≈ 7000 psi to ≈ 4500 psi for 200° and 300°C forgings, respectively. The strength loss with forging temperature was mildly affected by strontium content for dopant levels > 20 ppma, but below this strontium level Becher et al (1973) showed that the strength decreases rapidly with increase in annealing temperature. Changes in the strength-grain size behavior of KCl appear to result from deformation temperature effects on strength, also observed by Hendrickson et al (1973), and from dopant or impurity effects on recovery of residual strains (Becher et al, 1974a).

The loss in strength with increasing forging temperature corresponds with the reduction in the strain birefringence in the form of local banding, Figure 2, and an increase in plastic strain to failure, Table 1. Thus part of the increase in strength of alloys forged at 250°C (Becher et al, 1973) is a result of local residual strain hardening. Optimization of forging temperature must consider reduction of birefringence versus loss in strength, both of which occur by the recovery (or removal) of local residual forging strains. Annealing studies of recovery processes can aid in selecting the optimum forging temperature range. However, the forging temperature effects on microstructure, birefringence, and strength are needed as forging involves recovery during simultaneous deformation.

SUMMARY

Strontium-doped (≤ 1500 ppma) KCl crystals can be forged at temperatures ≤ 320°C to produce stable, fine-grained (~ 10μm) polycrystalline-like microstructures. The resultant strength and birefringence decrease with increase in forging temperature as recovery processes are enhanced. Optimumization of strength-birefringence behavior requires forging temperatures of ≥ 250°C for strontium addition of 500 to 1500 ppma.

REFERENCES

Anderson, R.H., Koepke, B.G., Bernal, G., E., and Stokes, R.J. (1973) J. Am. Ceram. Soc. 56:287.

Becher, P.F. and Rice, R.W. (1973), pp. 449-458 in Proc. High Power Infrared Laser Window Materials Conf., Vol. II, C.A. Pitha (ed.) AFCRL-TR-73-0372.

Becher, P.F., Freiman, S.W., Klein, P.H. and Rice, R.W. (1974a) pp. 579-600 in Proc. High Power Infrared Laser Window Materials Conf., Vol. II, C.A. Pitha, A. Armington and H. Posen (eds.) AFCRL-TR-74-0085.

Becher, P.F., Rice, R.W., Klein, P.H. and Freiman, S.W. (1974b) to be published in Proc. Deformation of Ceramic Materials Conf., R.C. Bradt and R.E. Tressler, eds., Plenum Press.

Bernal, G., E., Koepke, B.G., Stokes, R.J. and Anderson, R.H. (1973) pp. 413-448 in Proc. High Power Infrared Laser Window Materials Conf., Vol. II, C.A. Pitha (ed.) AFCRL-TR-73-0372.

Hendrickson, G.D., Starling, J.E. and Harrison, W.B. (1973) Interim Report No. 5, Contract F33615-72-C-2019, Honeywell, Inc.

Kulin, S.A., Neshe, P.P. and Kreder, K. (1974) pp. 637-673 in Proc. High Power Infrared Laser Window Materials Conf., Vol. II, C.A. Pitha, A. Armington and H. Posen, eds., AFCRL-TR-74-0085.

Mecking, H. and Kirch, F. (1971) pp. 257-288 in Recrystallization of Metallic Materials, F. Haessener, ed., Dr. Riederer-Verlag GmbH, Stuttgart.

Table 1. KCl FORGING PROPERTIES

Strontium added ppma	Temperature* °C	Strength		Permanent Outer Fiber Strain %	Grain Size μm
		Yield psi	Fracture psi		
1500	320[a]	4250	9000	1	15
1100	305[a]	4810	10000	1-2	8
200	310[a]	3700			8
670	280[a]	5067	11500	1-3	10
100	280[a]	4500			6
100	250[a]	3900			6
50	210[b]	≧7500		<0.1	7
	then annealed at 250	6600	8000	≧0.2	7

*Height reductions all ~65% to 75% in flowing He atmosphere.

[a]Slow cooled (~1°C/min from forging temperature to ~100°C).

[b]Fast cooled (~5°C/min).

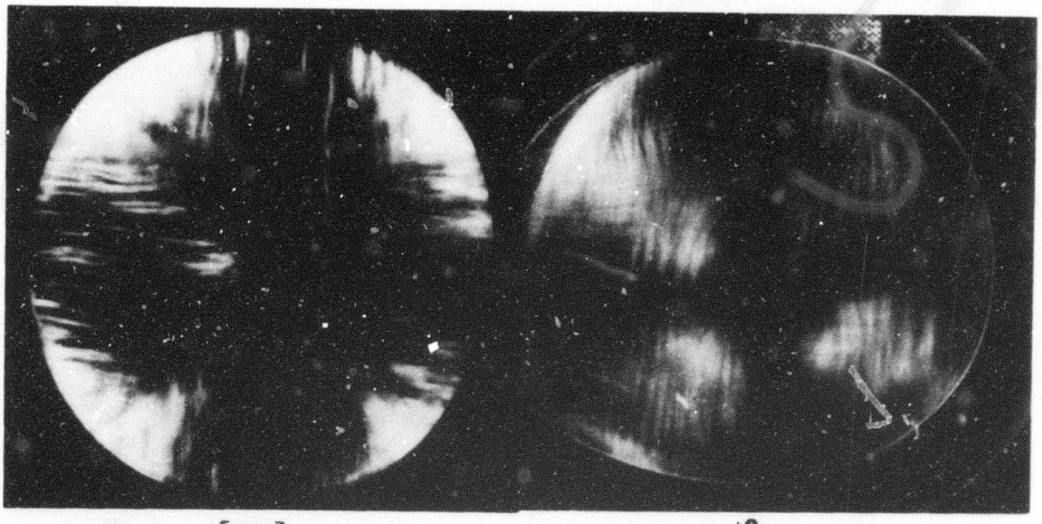

Pure [100] 200°C 65%

25ppma Sr^{+2} n[110] 270°C 65%

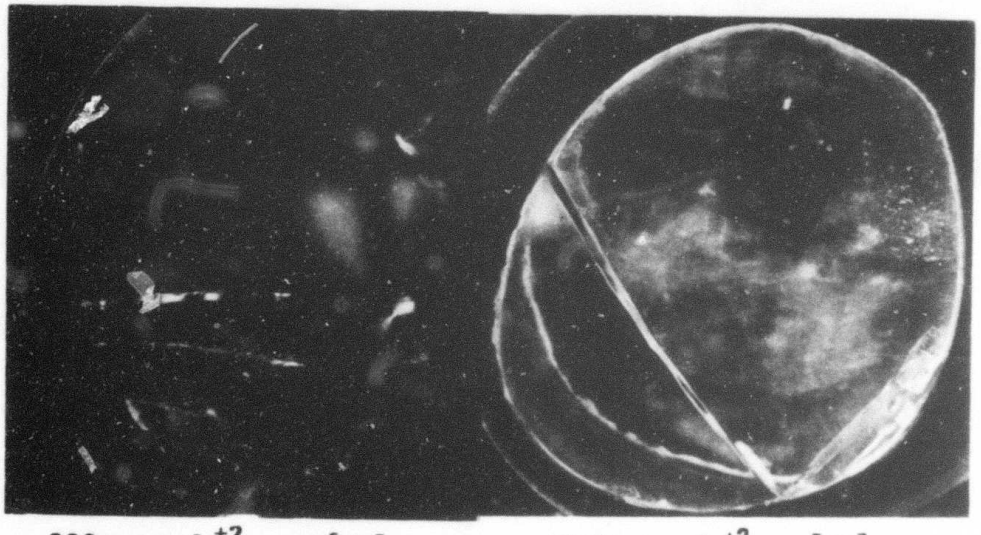

200ppma Sr^{+2} n[110] 310°C 75%

1500ppma Sr^{+2} n[110] 330°C 70%

Figure 1. Residual Birefringence Bands in KCl Forgings. The forging temperatures and height reductions are shown. The cracks in the lower forgings are a result of constraining ring failure or large flaws in original crystal. The only birefringence in these lower bodies is associated with the flaws.

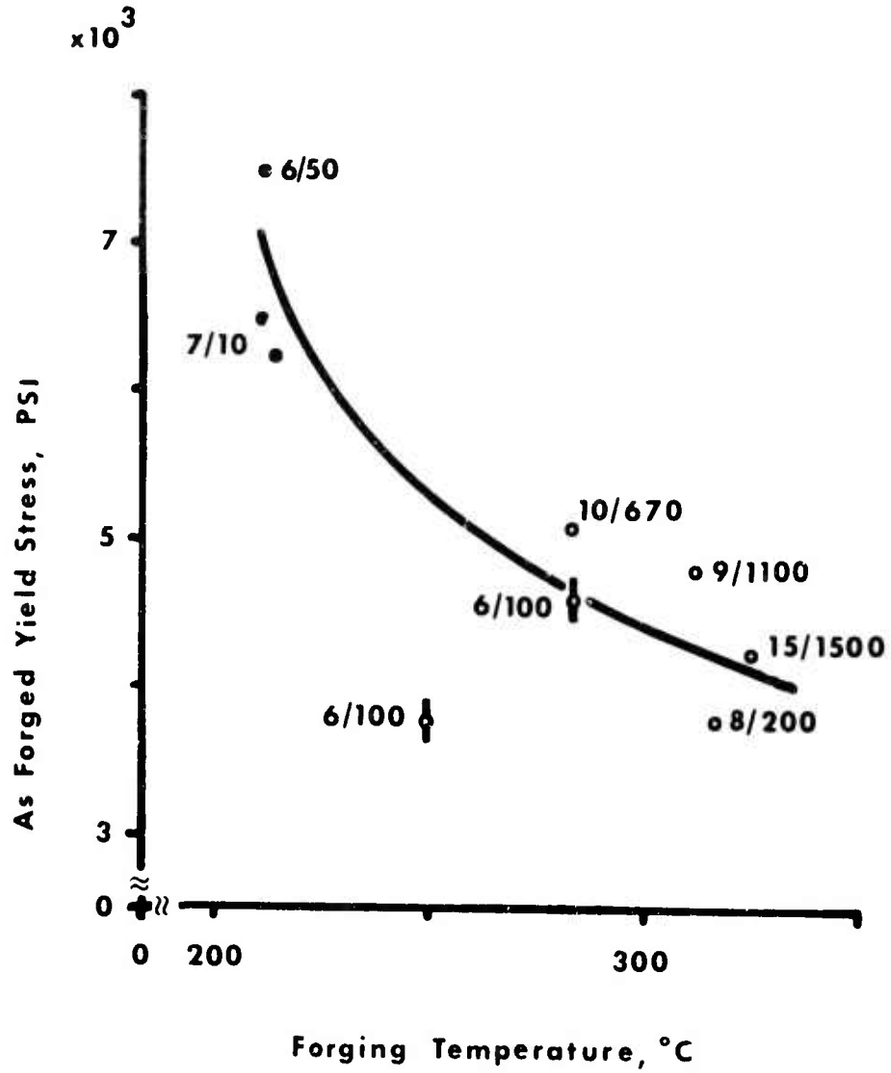

Figure 2. Strength Reduction in Higher Temperature Forgings. The degree of residual birefringence ranges from very high, inhomogeneous banding (●) to faint, parallel bands (ϕ) to uniform, weak birefringence (o). Grain size, microns/strontium added, ppma.

CRACK PROPAGATION IN KCl

S. W. Freiman, P. F. Becher and P. H. Klein
Naval Research Laboratory
Washington, D.C. 20375

1. INTRODUCTION

With the advent of high power 10.6μm lasers, it has become necessary to find materials with both low optical absorption and good strength for use as windows. Alkali halides such as KCl have very low absorption coefficients, but are very susceptible to cleavage and plastic deformation at low stresses. It was therefore important not only to strengthen this material but also to determine the influence of plastic deformation on crack propagation in order to find means to toughen it.

Studies of crack-dislocation interaction in materials such as LiF (Gilman, 1957) or Fe-3% Si (Tetelman, 1962) show that dislocations move out from the crack tip region, blunting the crack, thus inhibiting its propagation, and hence increasing fracture energy or toughness. In materials such as the alkali halides, the available $\{110\}\langle\bar{1}10\rangle$ slip systems intersect the preferred $\{100\}$ cleavage plane, as shown in Figure 1, and result in dislocation focusing at the crack tip to produce stress concentration or crack nucleation effects. Thus dislocation motion in the vicinity of the crack tip can inhibit crack propagation by blunting the crack tip, or aid crack motion by focusing dislocations to concentrate stress or nucleate sharp cracks at or near the existing crack tips. However,

there was no comprehensive understanding of these effects and the parameters affecting them was seen as a problem in laser window design. For example, large values of γ_c have been observed by previous investigators (Westwood and Hitch, 1963), but in most cases, these were discounted as being due to problems in experimental technique.

The objective of this study was to determine the relative role of {110} $\langle\bar{1}10\rangle$ slip in impeding and aiding {100} $\langle\bar{0}10\rangle$ crack propagation, and especially the dependence of fracture energy on critical resolved shear strength (CRSS) and strain rate. It will be shown that significant changes in fracture energy of single crystal KCl are observed and that these changes depend quite heavily not only on CRSS but also on loading rate and the crystal substructure. In addition, fracture energy was found to be consistently high in hot worked KCl. A mechanism explaining the observed variations in γ_c will be discussed and means of improving the toughness of these materials will be demonstrated.

2. EXPERIMENTAL PROCEDURE

Tests were performed on both commercial KCl crystals*, as well as crystals grown at NRL by the Czochralski technique, from melts containing 530-2000 ppma Sr^{+2}. Undoped crystals were tested both as-received and after γ irradiation to levels ranging from $1x10^6$ to $5x10^9$ Roentgens. Samples of both pure

---

*Harshaw Chemical Company, Solon, Ohio.

and Sr^{+2} doped KCl press-forged at NRL (Becher et al, 1974) and hot rolled KCl-KBr alloys* were also tested.

Specimens (≈ 6.5mm x 13mm x 50mm) were cleaved from single crystals and samples (≈ 2mm x 6.5mm x 50mm) were cut or cleaved from hot worked materials. The specimens were then chemically polished using water, followed by a solution of 2:1 acetic acid to alcohol, and then dried and stored in a desiccator. The hot worked materials were also longitudinally grooved, Figure 2, to produce a thickness of ≈ 0.5 to 1mm prior to polishing. Aluminum loading arms were cemented onto the specimen (Figure 2); just before testing, a {100} <001> pre-crack was introduced with a razor blade.

The test used in this study was a modification of the double-cantilever beam test in which a bending moment rather than a force is applied to the specimen (Freiman et al, 1973) (Figure 2). The primary advantage of this test configuration is the lack of dependence of measured fracture energy on crack length. In addition, this configuration eliminates the need to correct for shear and beam rotation effects. Fracture energy is obtained from the load and specimen geometry through the expression

$$\gamma = \frac{G}{2} = \frac{M^2}{2EIt}$$

where E is the elastic modulus in the crack direction; I is the moment of inertia of one side of the specimen

*Supplied by B. Koepke of Honeywell Research Corp., Bloomington, Minn.

about its longitudinal axis; t is the specimen thickness at the crack plane; M is the bending moment, PL; L is the fixed moment arm length; and P is the load on one arm of the specimen at which the crack is first observed to move and detected as a load drop in these tests. The tests were carried out in a universal test machine* at loading rates of 0.02, 0.2 and 5 cm/min. with the load (2P) being recorded on a strip chart. Subcritical crack growth was never observed in either the single or polycrystalline KCl specimens. When the critical load for a particular specimen was achieved, the crack popped forward quite rapidly. In the low yield stress materials, the crack eventually arrested, while in the heavily doped or irradiated, or polycrystalline, specimens, complete failure occurred. Most tests were carried out in 40-50% RH; some tests were performed in liquid N_2 by immersing the specimen in a beaker of the liquid. Many of the specimens were observed in circularly polarized light during testing. After testing, the specimens were analyzed in an optical microscope using polarized and phase-contrast light together with etching.

Yield strengths were measured on KCl bars (usually the halves of the fracture-energy specimens) in three-point loading using a conventional test machine** at strain rates comparable to those in fracture energy tests. The yield stress (=2 CRSS) was taken as the point at which the stress-strain curve departed from linearity (i.e., proportional limit).

---

* Instron Universal Test Machine, Instron Corp., Canton, Mass.

** Rhiele Universal Test Machine, Wilson Instrument Div., ACCO, Bridgeport, Conn.

3. RESULTS

The most important observation made during this study was the dependence of critical fracture energy on both CRSS and loading rate. At high rates of loading, 5 cm/min, fracture energy was independent of CRSS (τ_y) and low, Figure 2. The value of γ_c averaged 0.14 J/m^2 in pure, commercial KCl, comparable to that obtained by Class and Machlin (1966) (0.11) at 2.5 cm/min. At low loading rates (0.02 cm/min), extensive plastic deformation of the specimens occurred and cracks did not propagate. As soon as plastic deformation began, the load deflection curve deviated from linearity; the load eventually leveled off and remained constant until the test was stopped. Since linear elastic fracture mechanics obviously could not be used for these specimens, no fracture energy data was obtained.

The measurement of the γ_c of pure, commercial KCl at a loading rate of 0.2 cm/min yielded a value of 0.27 ± 0.04 J/m^2, which was insensitive to a variation in specimen thickness over the range 0.18 mm to ≈ 6.5 mm, or to changes in specimen width from 6.5 mm to 25 mm. This value of γ_c is significantly larger than the value of 0.11 J/m^2 reported by Westwood and Hitch (1963), who used an extrapolation technique in order to try and eliminate the effects of plastic blunting. Most of the load-deflection curves obtained at this loading rate were linear to just below the load at which crack propagation occurred. There was no correlation of the existence of a deviation from linearity with γ_c. The variation in γ_c with CRSS at 0.2 cm/min is shown in Figure 3. The curve is bimodal, with the difference between the two branches increasing

with CRSS up to about 10 MN/m^2, beyond which only low values of γ_c were observed. Gross and Gutshall (1965) observed a similar effect in NaCl. No difference in behavior was observed between irradiated and doped specimens or those tested in liquid nitrogen. Some single crystals were compressively prestrained 2%; the γ_c of these specimens at 0.2 cm/min was 0.8 J/m^2, compared to 0.27 J/m^2 for the unstrained specimens.

Under polarized light, slip bands were observed at the crack tip, whose intensity increased with increasing stress. The fact that plastic deformation has occurred in these bands is illustrated in Figure 4 by the dislocation etch pits and by the residual strain birefringence patterns on unloading which were identical to the plane strain patterns observed by Wiederhorn et al (1970). The orientation of the slip patterns is exactly what is expected because of the relationship of the cleavage plane in alkali halides to the {110} <110> slip system (Figure 1).

Evidence for crack tip blunting in the high γ_c specimens is given by the large shear lip and extensive river patterns seen on the fracture plane in Figure 5. These features should be contrasted with the relatively flat surfaces of the low γ_c specimen in Figure 5. It was also observed that the length of crack front blunting increased with increasing γ_c. No evidence of slip was found on crack fronts of specimens tested at 5 cm/min.

Figure 6 shows that for both press forged and hot rolled polycrystalline KCl, γ_c increases monotonically with yield stress, even though grain sizes varied from 5-10 microns and the specimens had varying degrees of texture. Evidence for plastic deformation in these

specimens was seen in the rounded edges and the number of slip lines on fracture surfaces. Also, previous laser testing (Rice, 1973) has shown that the plastic strain fields associated with crack propagation in polycrystalline KCl are similar to those observed in the fracture energy tests on single crystals.

4. DISCUSSION

The dependence of the fracture energy of KCl on both CRSS and loading rate can be explained on the basis of an interaction of the slip systems with the initially "sharp" crack as the stress at the crack tip is increased. An as-introduced crack in doped or irradiated KCl has negligible plastic deformation associated with it, as evidenced by the lack of slip lines when a crack was arrested and then propagated further with a razor blade. As the load is raised, the first process which occurs is the punching of edge dislocations from the crack tip or from sources in its vicinity. This is consistent with Gilman's (1958) observation that dislocation etch pits are always associated with crack fronts in rock salt structural materials and the work of Stokes (1962), who has shown that edge dislocations will propagate at stresses of about half the macroscopic yield stress in MgO. As these dislocation loops expand and move away from the crack, they relax the stress at the crack tip and/or physically blunt the crack. This blunting process is necessary to achieve the large values of γ_c on the upper curve in Figure 3. Without this process, cracks would propagate at γ_c's approaching the thermodynamic surface energy as the crack tip would remain relatively sharp.

If the edge dislocations are blocked by sub-grain boundaries or other local substructure, or there are insufficient mobile dislocations in the bulk, then no extensive crack blunting will take place, and fracture will take place at γ_c's associated with sharp cracks (lower curve in Figure 3). Evidence for this lack of blunting in these specimens is the absence of slip lines and lack of crack front lip (i.e., increase in crack tip radius) on the fracture surfaces of specimens which failed at these stress levels (Figure 5a).

The extent of crack tip blunting increases as the load is raised, making it increasingly difficult for the crack to propagate. In alkali halides (e.g., LiF), edge dislocation motion requires lower stress than for screw dislocations with comparable velocity (Johnston and Gilman, 1959). Extensive screw dislocation activity generally does not occur until the macroscopic yield stress is reached, as in the case of Fe-3% Si (Imura, 1972). Calculations of the bending stresses in the double cantilever arms in specimens with fracture energies along the upper curve in Figure 3 show that these stresses are $\geq$ two-thirds of the measured CRSS. The extensive plastic deformation, which takes the form of a large quantity of slip bands and shear steps, associated with the crack front in specimens having a high γ_c (Figure 5), is further evidence that the high γ_c is dependent on crack tip blunting. After edge dislocations propagate away from the tip and when the stress reaches the yield stress, screw dislocations can cross-glide onto parallel slip planes, resulting in dislocation glide back toward the crack tip. This produces a dislocation-focusing mechanism which causes failure in those specimens where blunting has produced a large γ_c,

and thus represents the upper limit of the fracture energy. The focusing mechanism could either involve the production of a "super <100> dislocation" at the crack tip by $<10\bar{1}>$ edge dislocation reactions, as theorized by Cottrell (1958) and recently suggested by Ahlquist (1973) to account for the increase in γ_c in rock salt crystals such as KCl, NaCl and MgO, or simply represent an additional stress concentration at the crack tip as suggested by Clarke et al (1962). Evidence favors the latter, for example, the $<10\bar{1}>$ dislocation reactions on orthogonal {110} planes are not energetically favored, as there is no lowering of dislocation energy in forming super <100> dislocations. As a result, it appears more likely that dislocation focusing increases the strain energy in the crack tip region, rather than forming <100> super dislocations. Also, if the crack direction is changed to a <011> in the {100} plane, the same γ_c-CRSS behavior is followed. Here, from the strain patterns observed at the crack tip, <110> dislocation appears to interact on 60° {110} planes. These would not react to form super <100> dislocations on the cleavage plane, and support the concept of stress concentrations due to dislocation glide to the crack tip region.

Both mechanisms could be expected to follow an expression of the form $\gamma_c \approx (\text{CRSS})^2$, which is shown as the solid curve in Figure 3. An interesting point with regard to this plot is that the data for pure KCl falls above the curve. The higher γ_c is probably due to the fact that in these soft crystals, a greater volume of material is easily plastically deformed upon introduction of the crack and applications of the load,

which would respectively reduce the effective crack tip stress and allow plastic energy to be absorbed in the arm.

Above a CRSS of $\approx$ 10 MN/m^2, the tendency to high γ_c's decreases precipitously. This reduction in γ_c is due to a decrease in the extent of blunting because of the much greater difficulty in moving even edge dislocations away from the crack tip (due to increased lattice resistance from high irradiation or dopant levels) before cleavage failure occurs from the sharp crack. At a loading rate of 5 cm/min, low γ_c's are always observed because at this high rate of loading, there is insufficient time for dislocation processes to effectively blunt the crack.

The fact that crack tip blunting so strongly affected γ_c suggests that if more sources of dislocations can be created within the crystals, such as by deformation of the specimens before testing, more blunting and higher values of γ_c would be obtained, at least at the intermediate loading rates. Further evidence is the increase in γ_c in deformed LiF specimens which was observed by Gilman (1960). Confirmation of this hypothesis was obtained by the larger value of γ_c obtained for KCl prestrained 4% before testing.

It appears that the greatest effect on the γ_c of polycrystalline KCl is the deformation structure formed during forging and which causes blunting at the crack tip as a result of the grain boundaries and dislocation substructure present.

5. SUMMARY AND CONCLUSIONS

Crack propagation, and therefore failure, in single crystals of KCl was shown to be strongly dependent on plastic deformation processes. A mechanism of crack tip blunting was described which led to high values of fracture toughness. The dependence of γ_c on CRSS and loading rates was also discussed. It was shown that crack growth in crystals having a high fracture toughness is due to a dislocation-focusing mechanism at the crack tip.

The single crystal toughness is quite variable, and improving the yield strength does not necessarily increase the fracture energy. In fact, under varying loading conditions, the fracture energy is always lowered by increasing the loading rates, a fact which must be considered in laser window design. It was shown that techniques such as prestraining of single crystals to introduce dislocations can be effective in achieving consistently high values of fracture toughness. The hot worked materials have high fracture toughness which is felt to be a result of the ease of crack blunting due to the presence of dislocation substructure.

ACKNOWLEDGEMENTS

The authors extend their thanks to B. G. Koepke of Honeywell Research Center for making the hot rolled KCl-KBr materials available. They also acknowledge M. Krulfeld of NRL for his aid in the crystal growth work, and J. Pfaff of NRL for irradiation of single crystals.

REFERENCES

Ahlquist (1973). Private communication and submitted to Acta Met.

Becher, P. F., Freiman, S. W., Klein, P.H. and Rice, R. W. (1974), pp. 579-600 in Proc. High Power Infrared Laser Window Materials Conf., Vol. II, C. A. Pitha, A. Armington, and H. Posen, (eds.), AFCRL-TR-74-0085.

Clarke, F. J. P., Sambell, R. A. J. and Tattersall, H. G. (1962). Phil. Mag. 7:393.

Class, W. H. and Machlin, E. S. (1966). J. Am. Ceram. Soc. 49:306.

Cottrell, A. G. (1958). Trans. AIME 212:192.

Freiman, S. W., Mulville, D. R. and Mast, P. W. (1973). J. Matls. Sci. 8:1527.

Gilman, J. J. (1957) Trans. AIME 209:449.
(1958) Trans. AIME 212:310.
(1960) J. Appl. Phys. 31:2208.

Gross, G. E. and Gutshall, P. L. (1965). Int. J. Fract. Mech. 1:131.

Imura, T. (1972), pp. 104-133 in Electron Microscopy and Structure of Materials, G. Thomas, R. M. Fulrath and R. M. Fisher, eds., Univ. of California Press, Berkeley.

Johnston, W. G. and Gilman, J. J. (1959). J. Appl. Phys. 30:129.

Rice, R. W. (1973). Semi-Annual Report No. 3, ARPA Order 2031, Naval Research Laboratory.

Stokes, R. J. (1962). Trans. AIME 224:1227.

Tetelman, A. S. (1963), pp. 461-501 in Fracture of Solids, D. C. Drucker and J. J. Gilman, eds., Gordon and Beach, New York.

Westwood, A. R. C. and Hitch, T. T. (1963). J. Appl. Phys. 34:3085.

Wiederhorn, S. M., Moses, R. L. and Bean, B. L. (1970). J. Am. Ceram. Soc. 53:180.

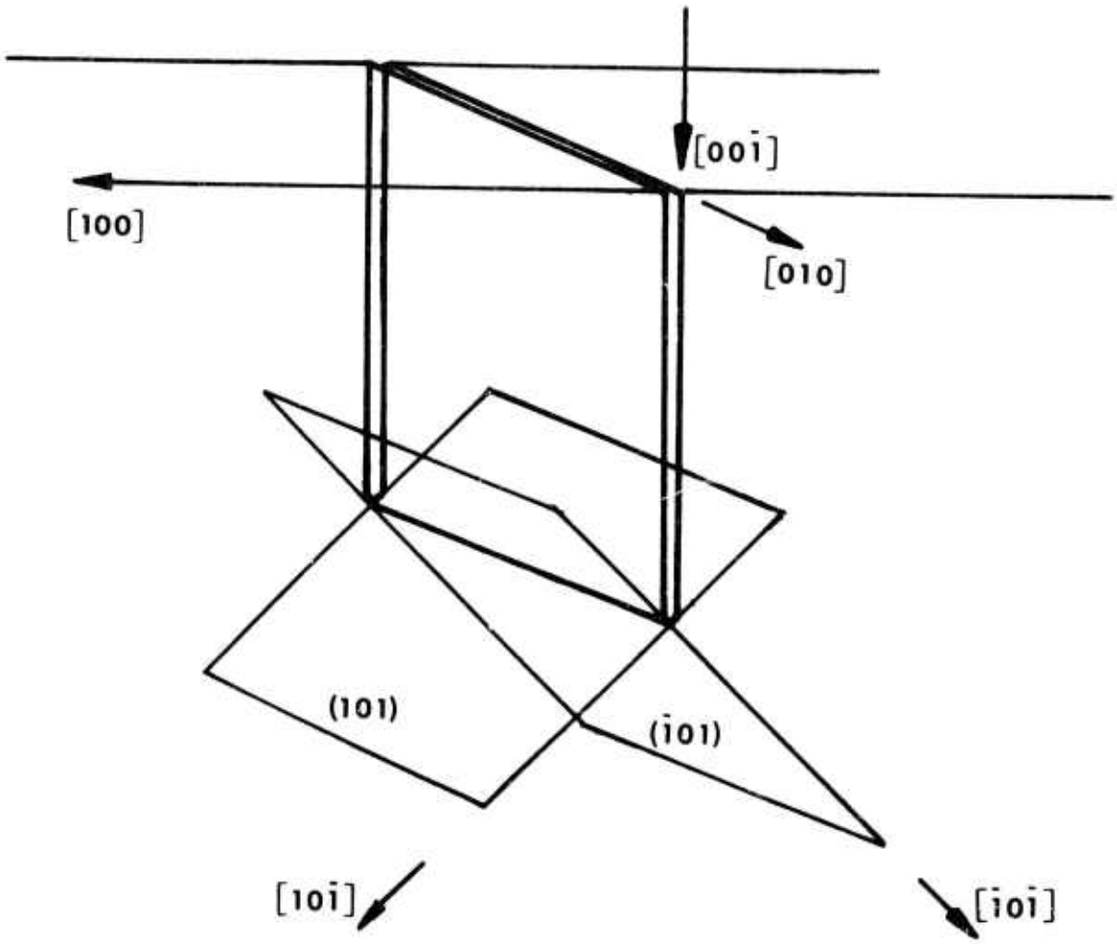

Figure 1. {101} <10$\bar{1}$> Slip Systems Which Intersect {100} Cleavage Crack in Fracture Energy Tests.

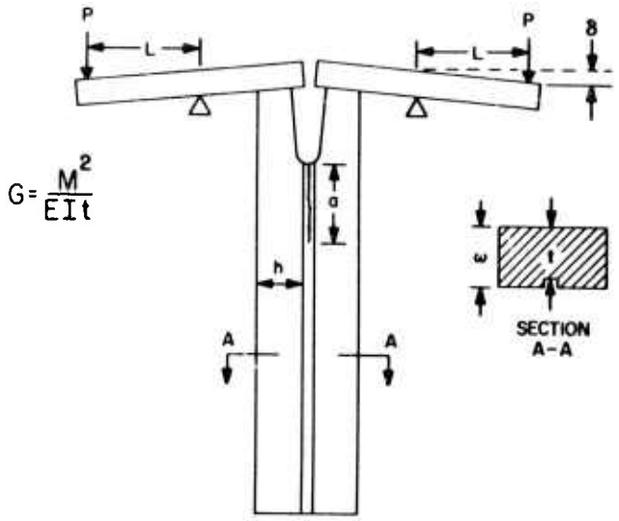

Figure 2. Fracture Energy Test Configuration. Hot worked materials were grooved as shown, while single crystals did not require groove.

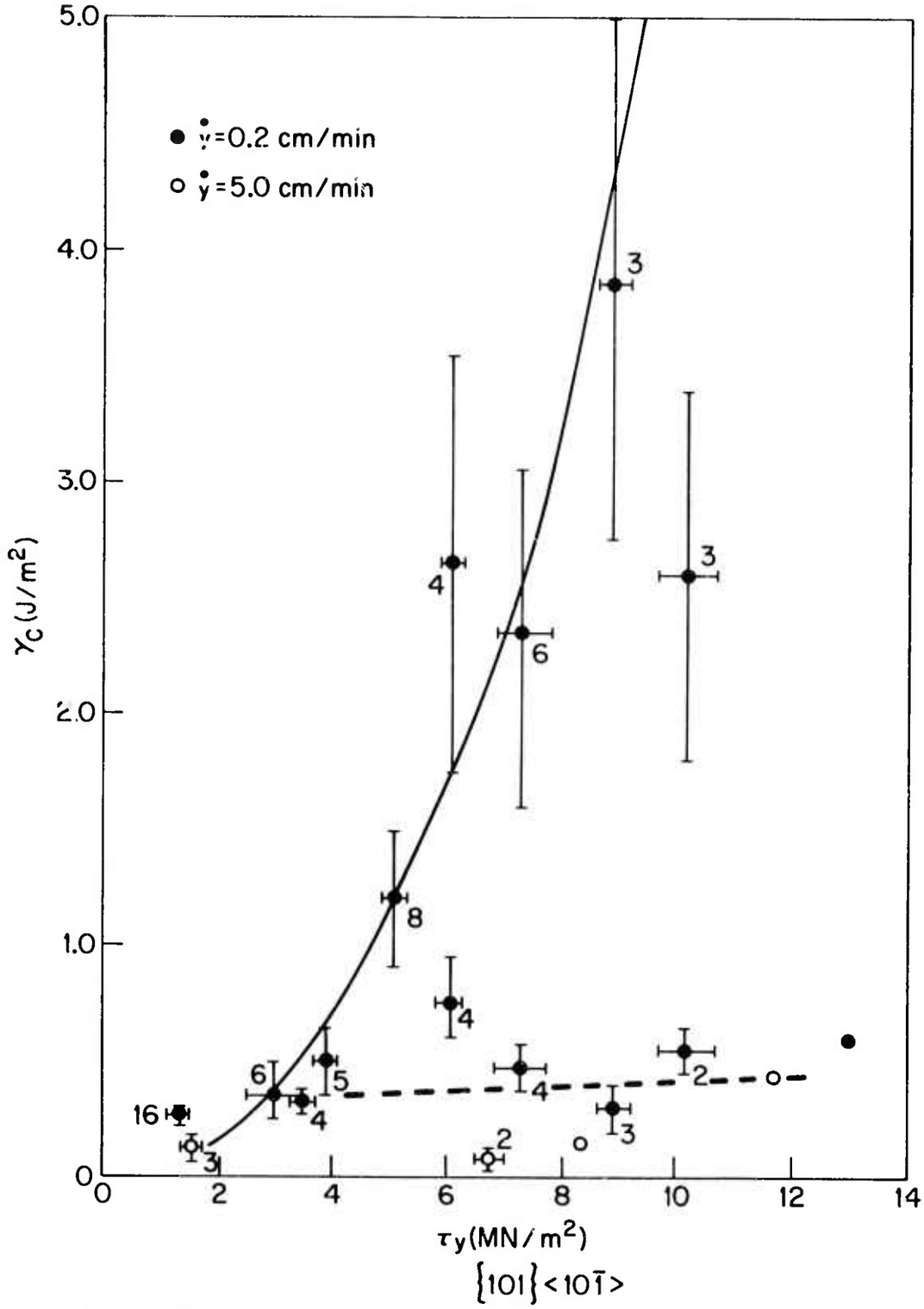

Figure 3. Fracture Energy - Critical Resolved Shear Stress Behavior in KCl Single Crystals.

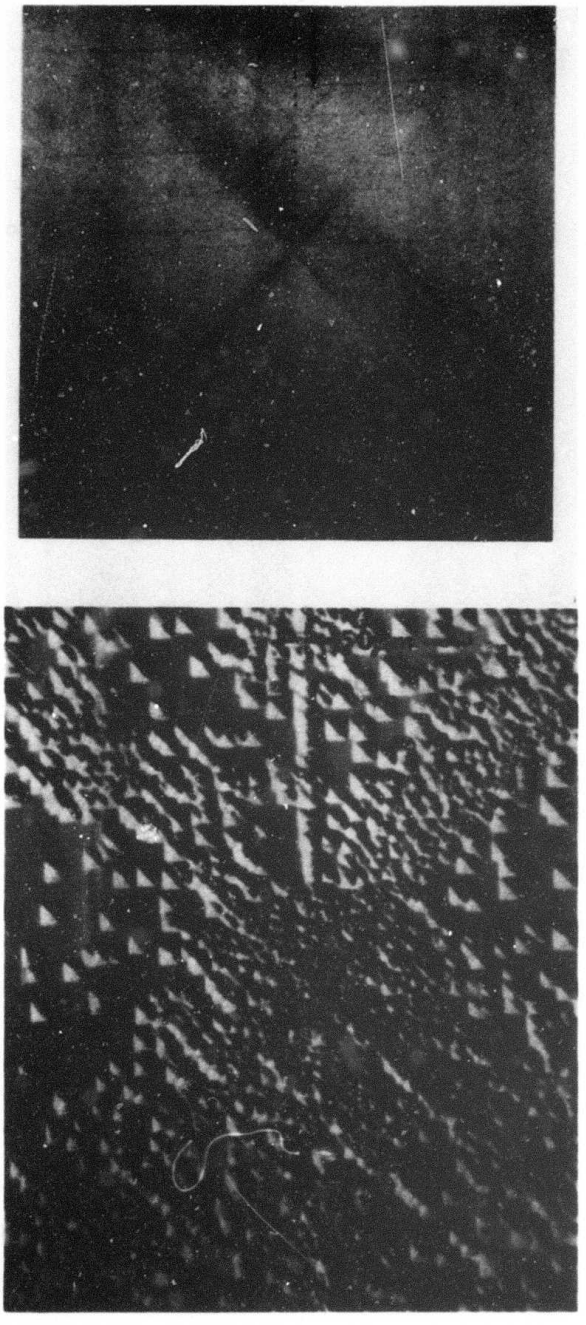

Figure 4. {101} Slip Bands at {100} Crack in Fracture Energy Specimens. KCl single crystal (top) shows slip systems viewed normal to crack plane; dislocation etch pits on slip bands at crack tip in NaCl (bottom).

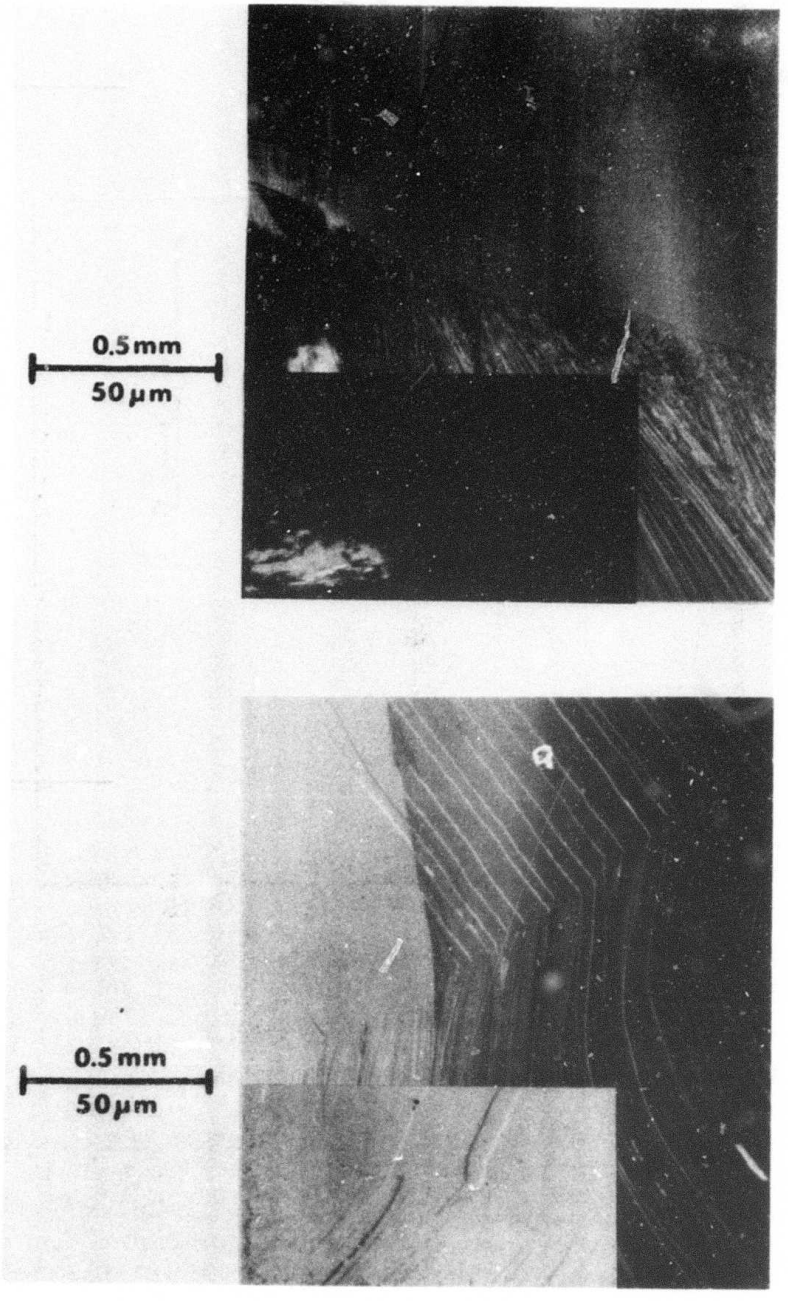

Figure 5. Crack Front Deformation in KCl Crystals. Top: Insert shows dark slip lines at crack front for material with γ_c = 2.7 J/m^2 and τ_y = 7 MN/m^2. Bottom: Absence of blunting and slip at crack in crystal with γ_c = 0.5 J/m^2 and τ_y = 7 MN/m^2.

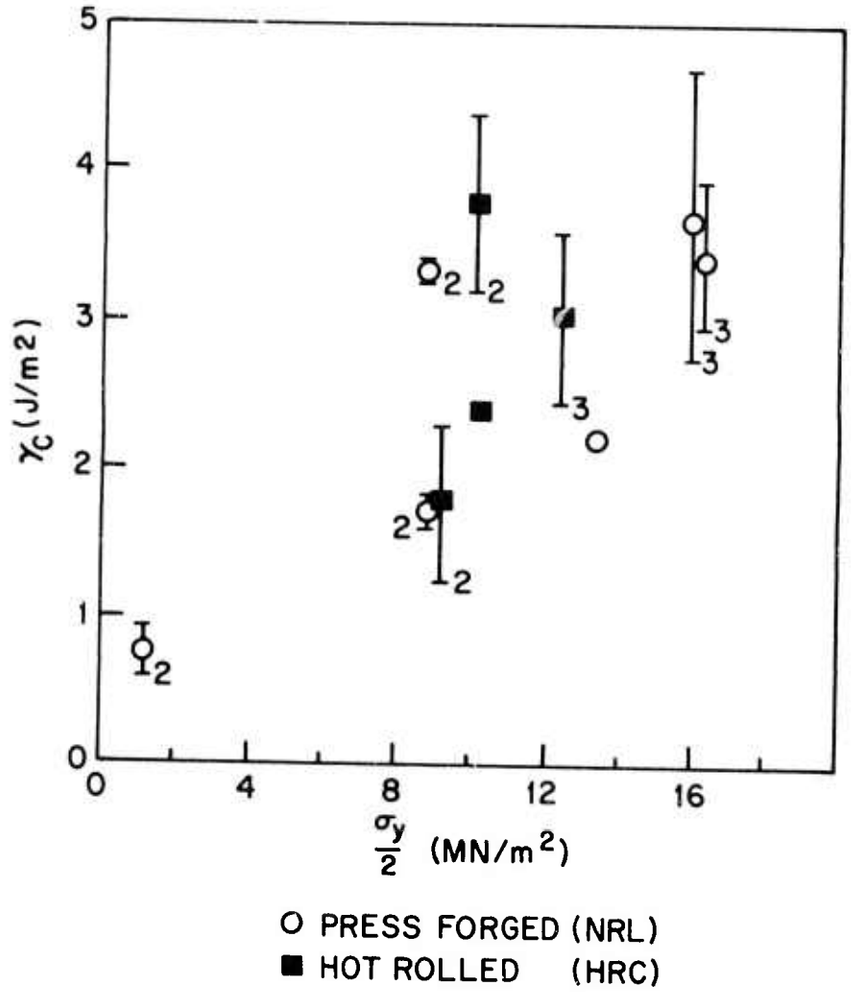

Figure 6. Fracture Energy of Hot Worked KCl as a Function of Yield Stress.

10.6μm IRRADIATION DAMAGE IN PRESS FORGED KCl

P.F.Becher, R.W.Rice, J.J.Mecholsky, and J.R.Spann
Naval Research Laboratory
Washington, D.C. 20375

1. INTRODUCTION

The initial laser tests conducted in this program showed that significant plastic deformation developed in the samples during irradiation (Rice, 1973). In a forged pure KCl window, pre-existing flaws led to intermittent crack growth during irradiation as a result of plastic deformation at crack tips. The present work compares laser tests of low absorption single crystal forgings having different strengths and residual birefringence.

2. EXPERIMENTAL

Uncoated, chemically polished samples (1"x1"x0.15") of both pure and strontium-doped KCl forgings were tested, including samples with various degrees of residual forging birefringence banding. The surface finish, which was generally uniform among specimens, was not optimized for minimum absorption, but total absorption was estimated to be $\leq 1 \times 10^{-3} cm^{-1}$. The CO_2 test laser had a 6mm diameter, top hat beam, and delivered a power density of 18 KW/cm^2 to the target for $\approx$ 6 seconds per run. Changes in strain birefringence in the samples during irradiation were recorded by a movie camera (200 frames/sec) using transmitted polarized lighting of the sample. Comparison of the strain birefringence in the samples before and after irradiation was used to detect any permanent deformation introduced.

3. RESULTS AND DISCUSSION

The pure samples, Figure 1, have not fractured, but they did exhibit local plastic deformation in the region of the transmitted beam. This localized plastic deformation is a result of the lower yield strength of the pure forgings. Greater deformation damage occurred in the <100> axis forgings as the beam transmitted through the intersection of two {110} deformation band sets where the residual forging strain is highest. Though damage occurred in the pure near <110> axis KCl forging, it does not appear to be as extensive. The strength of this forging is comparable to the <100> forgings; the decreased damage is consistent with the absence of intersecting birefringence bands and less extensive birefringence in this <110> forging. Neither of the two near <110> axis, strontium-doped forgings, Figure 1, exhibit any laser-induced plastic deformation, regardless of the presence of residual forging strain banding. The flaw in the strain-free strontium-doped forging was one present in the surface prior to irradiation. The interesting point is that due to the high fracture toughness of such forged materials, this flaw grew only slightly and stopped, even after three irradiation cycles of $\approx$ 6 seconds each. Laser-induced crack growth in forged pure KCl was observed to be more extensive during a previous single cycle test (Rice, 1973).

4. CONCLUSIONS

These tests, with a 6mm diameter, 18 KW/cm^2 beam, indicate that the incidence of damage in the form of laser-induced plastic deformation diminished with

increasing yield strengths above 3000 psi, and increased with increasing residual strains and related birefringence. Inherent surface or bulk flaws can grow during irradiation, but forged or hot worked materials are very resistant to crack growth, consistent with the fracture energy behavior discussed by Freiman et al (1974) in this report.

REFERENCES

Freiman, S.W., Becher, P.F., and Klein, P.H. (1974). Semi-Annual Report No. 4, ARPA Order 2031, Naval Research Laboratory.

Rice, R.W. (1973). Appendix, Semi-Annual Report No. 3, ARPA Order 2031, Naval Research Laboratory.

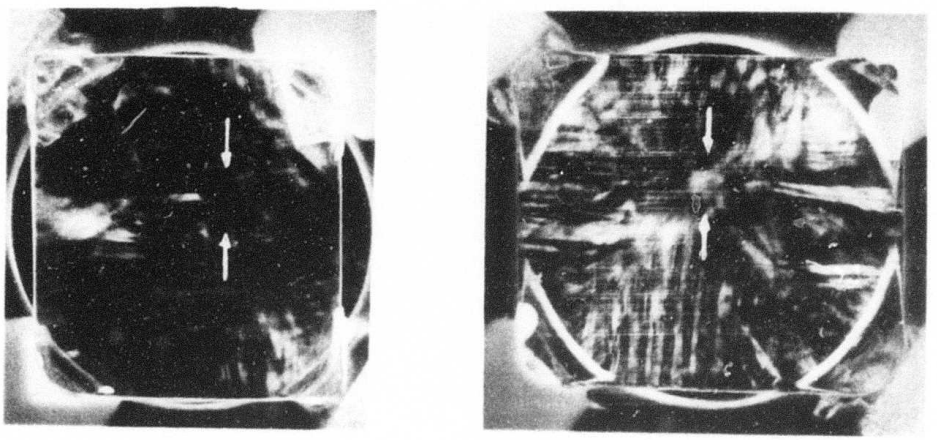

230°C
61%

Pure
S.C. $\beta = 6 \times 10^{-4}$/cm
$\sigma_y = 2500 - 3000$ psi

250°C
54%

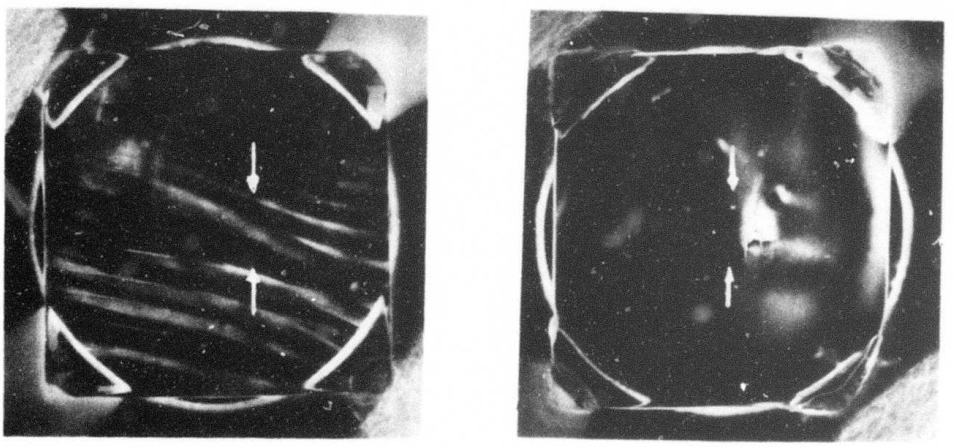

225°C
57%
$\sigma_y \approx 5000$ psi

$\simeq 100$ ppma Sr^{+2}
S.C. $\beta \leq 2.5 \times 10^{-4}$/cm

305°C
72%
$\sigma_y = 3850$ psi

Figure 1. Laser Damage in Press Forged KCl. Upper. Pure KCl forgings: <100> forging (right); n<110> forging (left). Lower. n<110>, strontium-doped KCl forging: With residual birefringence banding (left); free of banding (right). Arrows indicated region beam transmitted.

FRACTURE OF ZnSe AND As_2S_3*

R. W. Rice, S. W. Freiman and J. J. Mecholsky, Jr.
Naval Research Laboratory
Washington, D.C. 20375

and

J. C. Wurst**
University of Dayton
Dayton, Ohio 45409

1. INTRODUCTION

Materials such as ZnSe, which fracture in the absence of any macroscopic plastic deformation, may fail from flaws which have a statistical distribution of size and location. Such flaw distributions result in strength distributions which must be accounted for in any design for mechanical loads. However, the particular design criteria used depends on the types of flaw location, e.g., whether they are on the surface, in the bulk, or both. NRL has developed an extensive capability for locating and characterizing the exact fracture origins in many materials. This expertise was applied to CVD ZnSe specimens whose mechanical behavior is being studied at the University of Dayton (UOD) to determine the origin and character of fracture initiation in some of their mechanical test specimens. Initial results of this work are reported below.

* This work was not done under ARPA contract, but is reported here for the convenience of those concerned with laser windows.

** Work performed under AFML Contract No. F33615-72-C-1257.

Determining the strength of specimens provides a baseline for mechanical design. However, it is normally necessary to also measure crack propagation parameters. Fracture energy measurements determine the energy required for crack propagation under loading conditions that cause catastrophic failure. Such information can be used to calculate flaw sizes, and to determine the extent that a crack will grow under a local stress which is insufficient in spatial extent to cause complete mechanical failure of the part. Such crack growth then causes a decrease in strength due to stress-history dependence. Fracture energy measurements in ZnSe and As_2S_3 are reported below.

Slow crack growth, that is, growth below stress levels associated with catastrophic failure, results in an even greater stress-history dependence of strength. If such growth occurs, then either of two routes must be followed. Either crack velocity as a function of stress intensity, K, at the crack tip must be determined, or, if it is possible, the cause of the slow crack growth must be eliminated. Initial results demonstrating slow crack growth in both ZnSe and As_2S_3 are reported.

2. EXPERIMENTAL PROCEDURE

Nine CVD ZnSe and one PVD ZnSe rectangular cross section-flexure bars previously tested by the UOD (Wurst and Kuhl, 1974) were examined. All were highly polished with rounded edges. Three CVD ZnSe double cantilever specimens (≈ 2"x0.25"x0.125") (see Figure 2, Freiman et al, 1974) were prepared at the UOD and tested at NRL. Arms of the fractured double cantilever specimens were then flexure-tested at NRL and examined for fracture origins.

As_2S_3 glass plates* were machined into bars (~0.1"x0.2" cross section), were ground with a 180 grit diamond wheel, and tested in flexure with the grinding striations either parallel or perpendicular to the tensile axis. Specimens were examined for fracture origins. Double cantilever beam specimens (~1/2"x2"x0.04") were similarly machined from As_2S_3 plates.

Fracture origins were determined optically and characterized as described by Rice (1973a). Fracture energies were measured by the modified double cantilever beam technique of Freiman et al (1973).

3. RESULTS AND DISCUSSION

3.1. Strength and Fracture

The strength and fracture origin data of UOD and NRL-tested ZnSe are shown in Table 1. The significant number of fracture origins at the corners of the fracture surfaces (i.e., the edges of the specimens) indicates a significant edge finishing problem common to many ceramics (Rice, 1973b). This could be quite important to laser windows, since significant stresses may occur at the edges. These results indicate only surface failures, but the flexure test biases failure to the surface. Results discussed below indicate that some volume sources of failure may have to be considered.

Preliminary characterization of fracture origins is also given in Table 1 and Figures 1-4. Figure 1 is typical of several corner and tensile surface failures from regions having spalled or irregular areas at or near the fracture origin. Figure 2 shows optical photos of

---

*Servo Corporation of America, Hicksville, N.Y. 11802.

two specimens indicating origins from possible flaws of about 30-50μm deep, which is of the same order of apparent flaws in other samples. Such a range of sizes is about one-fourth of that calculated from the fracture energies of Table 2, assuming penny-shaped flaws. This discrepancy could well arise from the flaws being in only one or two grains, so single crystal fracture energies may be more applicable for use in the Griffith equation to calculate strengths or flaw sizes, as suggested by Rice (1974) and Freiman et al (1974).

The effects of larger grains on fracture initiation are indicated in Table 1, Figure 2, and especially Figure 3. Since mechanical failure seeks out the weakest link, and large grains are a preferred source of failure, a volume distribution of such large grains could mean a volume distribution of failure sources. Further, since the failure in Figure 3 appears to originate from the pore near the corner, such pores could also lead to volume sources of failure.

Figure 4 shows fracture features on the one PVD sample studied thus far. This sample failed from a grain boundary surface, but had mostly transgranular failure elsewhere. (All the CVD samples had virtually 100% transgranular failure.) Dots on the grain surfaces indicate pores and/or precipitates, while the linear features presumably represent twins. Whether the twins are due to processing or stressing is uncertain, but they, along with the pores, are probably factors in the intergranular failure, and possibly fracture initiation. If the latter is true, this would again indicate volume sources of failure. (Note linear features suggestive of twins were also observed in the large grains near the fracture origin of the specimen of Figure 3.)

As_2S_3 specimens ground parallel to the tensile axis had average strengths of about 3000 psi, while specimens ground perpendicular to the tensile axis had average strengths of about 2700 psi. Fractures originated from machining-induced flaws (Rice, 1974, and Mecholsky, et al, 1974).

3.2. Crack Propagation

Initial fracture energy measurements on both As_2S_3 and ZnSe are shown in Table 2. The fracture energies of As_2S_3 have been corroborated by measurements of characteristic fracture mirror sizes (Mecholsky et al, 1974).

Initial data in Figures 5 and 6 show that slow crack growth does indeed occur in both As_2S_3 and ZnSe. Tests are under way to determine whether environmental factors, especially H_2O, are responsible for this, as in many other materials, or whether other processes, such as microplasticity (e.g., in ZnSe), are involved. Preliminary data indicate that crack velocities at a given K are higher in H_2O than in air. The results show that the strengths of bulk ZnSe and ZnSe or As_2S_3 coatings for laser windows are stress-history and environment-sensitive.

4. SUMMARY AND CONCLUSIONS

Fracture origin and crack propagation studies of polycrystalline ZnSe and glassy As_2S_3 have been initiated. A significant number of edge failures in ZnSe emphasize the importance of edge flaws in windows where edge stresses may be high. While bend tests of ZnSe gave only surface failure, association of such failures with processing defects such as large grains, pores, and

possibly twins, indicate that volume sources of failure may have to be considered. Fracture energies of As_2S_3 are about 2 J/m^2, while initial ZnSe results have been scattered in the 3-6 J/m^2 region. Flaw sizes calculated from these ZnSe values are about fourfold larger than fractographically indicated flaws. This suggests flaws may commonly be contained in one or two grains with single crystal fracture energies being more appropriate. Finally, both As_2S_3 and ZnSe exhibit slow crack growth, which indicates that their strengths may well be stress-history and environmentally dependent.

REFERENCES

Freiman, S.W., Mulville, D.R. and Mast, P.W. (1973). J. Matl. Sci. 8:1527.

Freiman, S.W., McKinney, K.R. and Smith, H.L. (1974). pp. 659-676 in Fracture Mechanics of Ceramics, R. C. Bradt, D. P. H. Hasselman and F. F. Lange, eds., Plenum Publishing Corp., New York.

Mecholsky, J. J., Rice, R.W. and Freiman, S.W. (1974). Accepted for publication in J. Am. Ceram. Soc.

Rice, R.W. (1973a) to be published in the Proceedings of the Symposium on Surfaces and Interfaces in Glass and Ceramics, held at Alfred University.

Rice, R. W. (1973b) to be published in the Proceedings of the Symposium on Ceramics for High Performance Application held at Hyannis, Mass.

Rice, R. W. (1974), pp. 323-346 in Fracture Mechanics of Ceramics, R. C. Bradt, D. P. H. Hasselman and F. F. Lange, eds., Plenum Publishing Corp., New York.

Wurst, J.C. and Kuhl, G.B. (1974), pp. 733-745 in Proc. High Power Infrared Laser Window Materials Conference, II, C. A. Pitha, A. Armington and H. Posen, eds., AFCRL-TR-74-0085.

Table 1

ZnSe FRACTURE ORIGINS

Specimen No.	Flexure Strength (1000 psi)	Fracture Origin
A. University of Dayton Tests:		
61-C-41-1	5.58	From surface of chip or spall on tensile surface, possibly from flaw ~10μm deep at edge of chip or spall.
60-1	4.42	Tensile surface near corner. Possible chip ~15μm deep.
60-2	5.98	Corner (see Fig. 1).
96-3B	5.16	Tensile surface.
96-2B	3.51	Tensile surface.
94-8D	8.48	Most likely corner, possibly from smaller grains next to larger grains just inside of surface.
82-6	8.41	Corner.
61-C-24-4	4.86	Corner - very large grains with pore (see Fig. 3).
ZnSe-5a-2[1]	4.8	Grain boundary surface ~ normal to tensile surface (see Fig. 4).
B. NRL Tests:		
1	7.31	Corner.
2	8.09	Tensile surface.
3	7.31	Tensile surface.
4	8.51	Corner (see Fig. 2).
5	7.03	Tensile surface (see Fig. 2).

[1]PVD material; all other specimens are CVD material.

Table 2

FRACTURE ENERGIES

Material	Fracture Energy (J/m^2)
As_2S_3	2
ZnSe	3-6

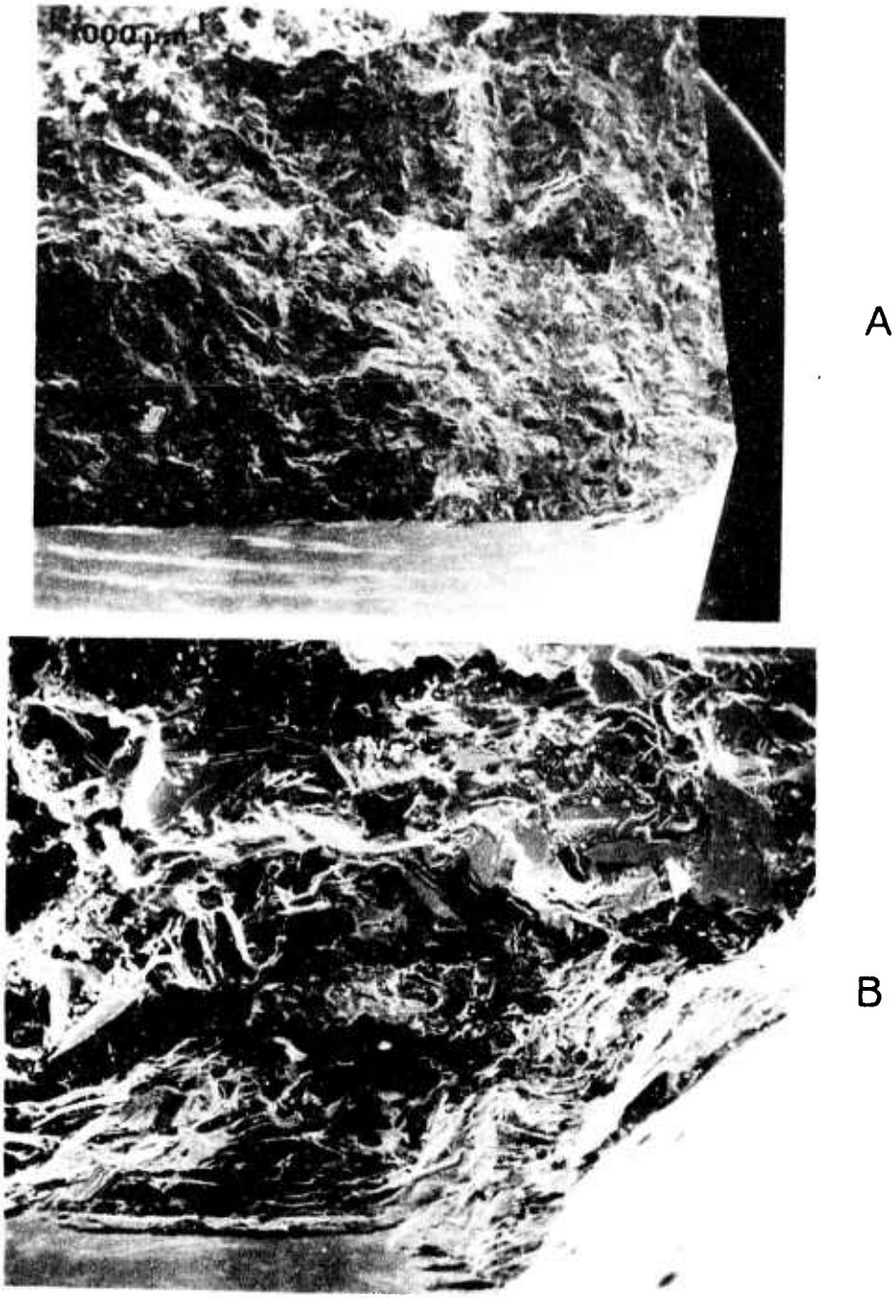

1. SEM of CVD ZnSe. UoD fracture (60-2) showing typical corner fracture origin. Note also chipping or spalling at or near corner and origin typical of several origins including some from the tensile surface.

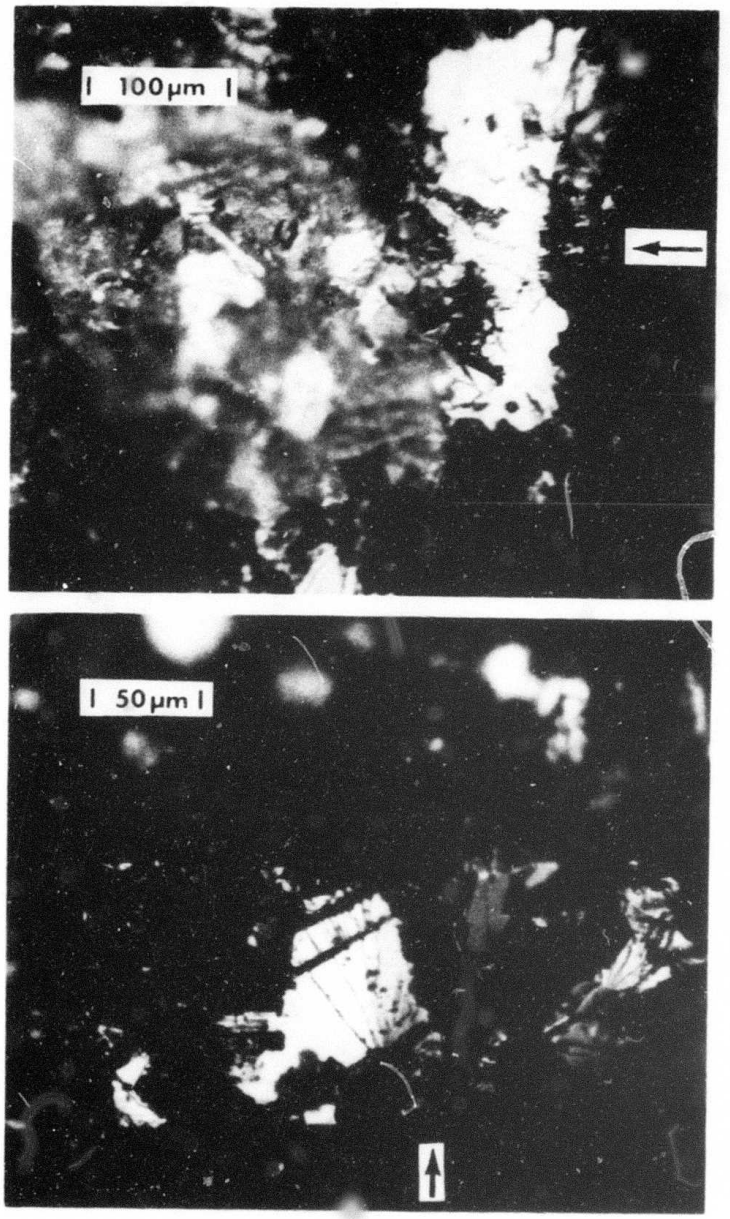

2. Optical photos of fracture origins in two CVD ZnSe specimens. A - NRL test No. 4 failing from a corner. B - NRL test No. 5 , failing from a tensile surface. Note flaw-like features at both origins (arrows).

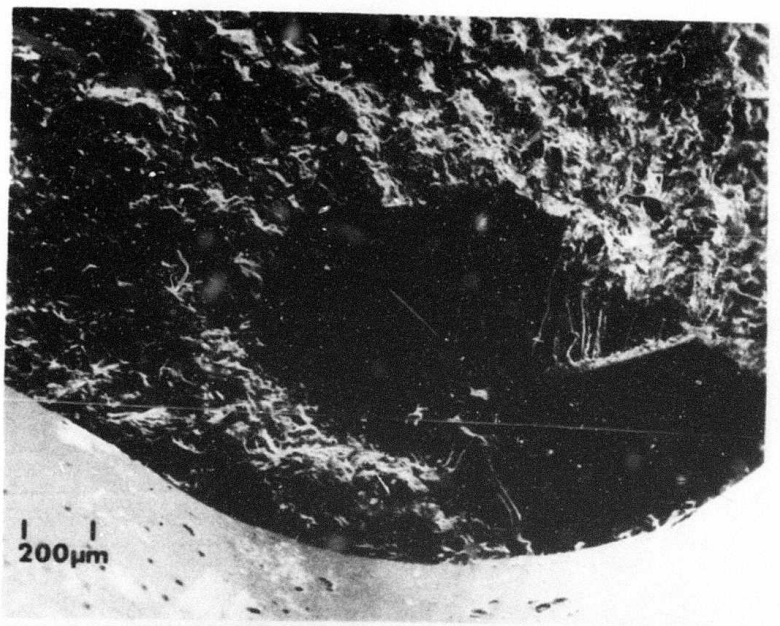

A

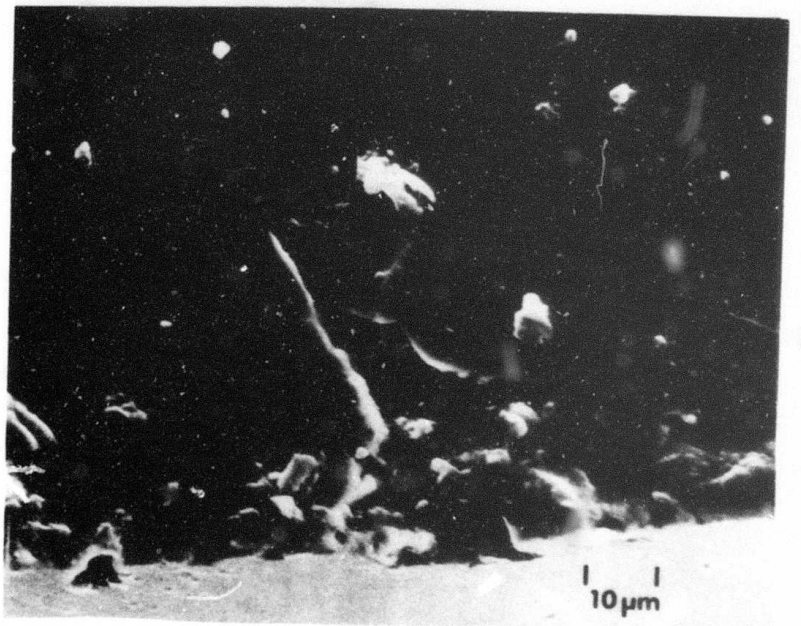

B

3. SEM of CVD ZnSe. UoD fracture (61-C-24-4). Note failure from three unusually large grains at corner. Fracture appears to initiate from void partially exposed by edge finishing (B).

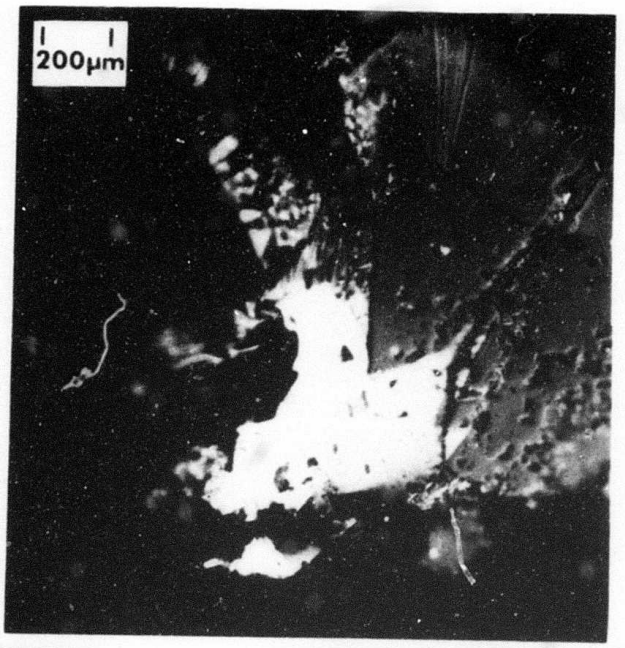

A

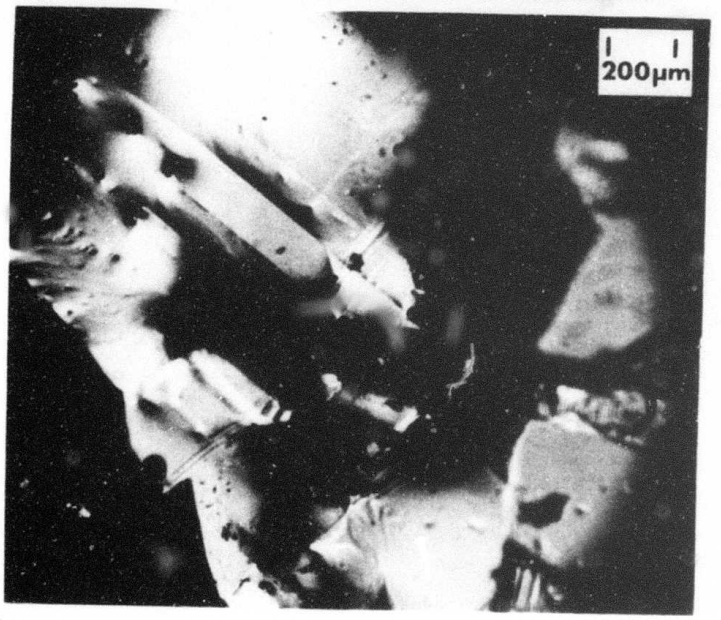

B

4. Optical photos of PVD ZnSe. A - Fracture origin from grain boundary surface (mostly white area). B-Nearby internal region of intergranular fracture. Note linear features in both A & B indicating twins and dots indicating voids or percipitates.

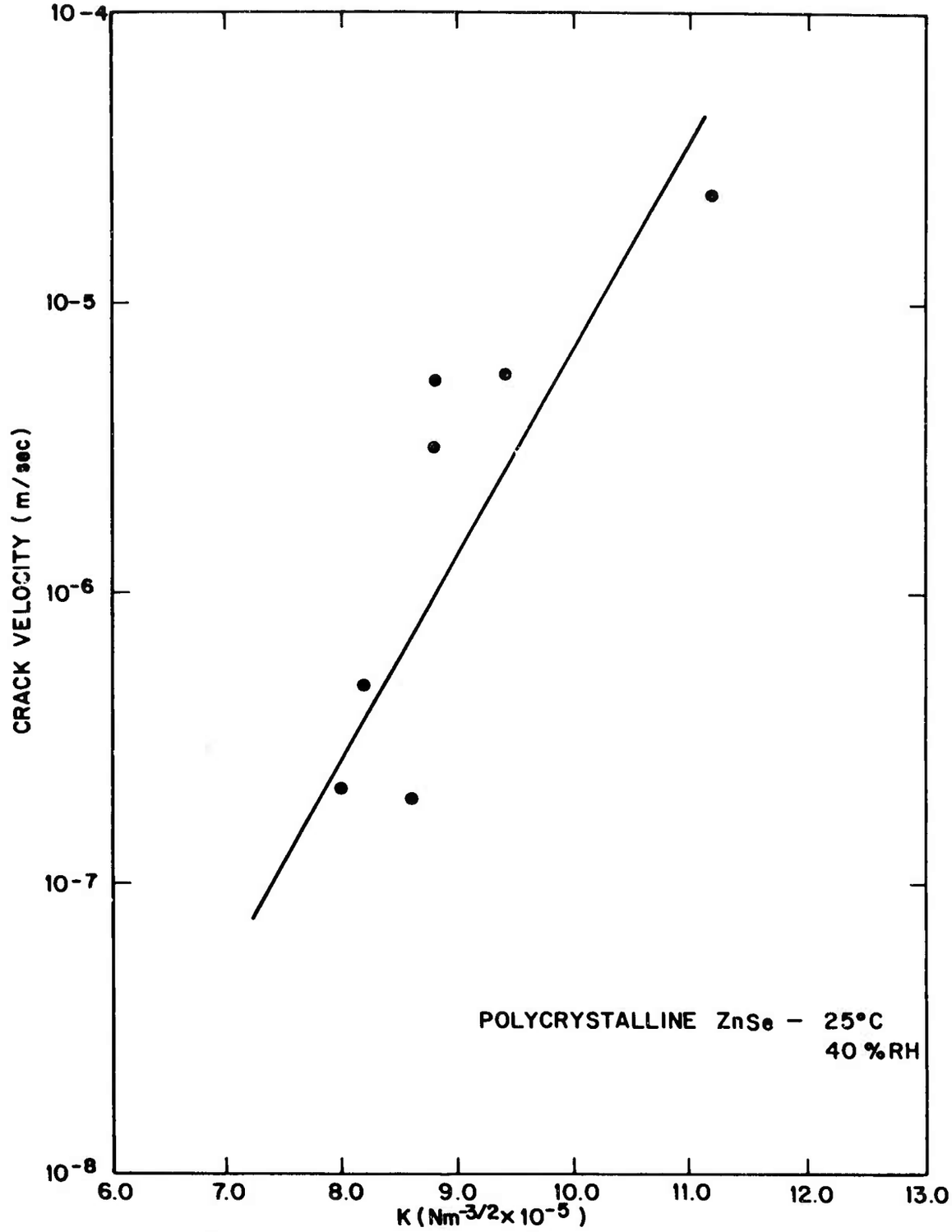

5. Crack velocity versus stress intensity in ZnSe. This shows slow crack growth occurs.

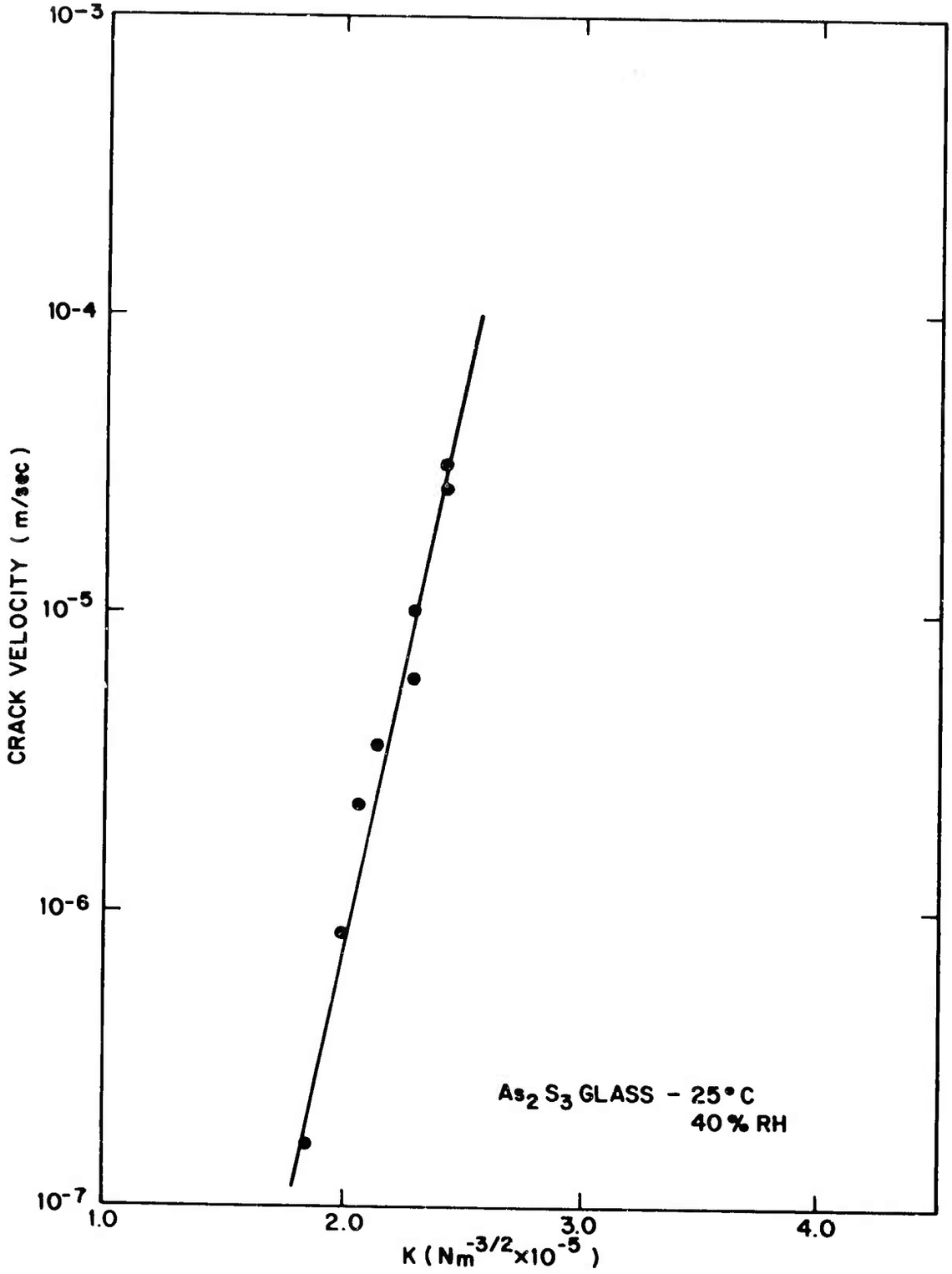

6. Crack velocity versus stress intensity in As_2S_3. This shows slow crack growth occurs.

THEORY OF INTRINSIC MULTIPHONON ABSORPTION AND COMPARISON WITH EXPERIMENT

Larry L. Boyer and
Herbert B. Rosenstock
U.S. Naval Research Laboratory
Washington, D.C. 20375

A long range objective of the laser window program at NRL has been the understanding of the origin of the absorption in candidate materials. As the purity of materials has improved, the impurity absorption has decreased. As a result, in KCl, which has the lowest total absorption of any known material at 10.6 μm, an appreciable portion of this residual absorption can be attributed to intrinsic multiphonon absorption. For this reason, a detailed theoretical and experimental study of the frequency and temperature dependence of multiphonon absorption has been carried out at the Naval Research Laboratory. A manuscript describing these investigations will be prepared in the next few months for submission to a scientific journal. In this present report, attention will be focused on the major achievements and problems in the reporting period.

Experimental results[1,2,3] suggest the following general picture of the frequency and temperature dependence of multiphonon absorption in alkali halides. Except for some two-phonon structure the frequency dependence follows the empirical law

$$\beta = A\, B^{(\Omega/\omega_m)} \qquad (1)$$

where Ω is the frequency of the light, ω_m is the maximum frequency of the solid and A and B are constants which depend only on T. For a large number of materials the room temperature value of B is $0.01 \pm 50\%$ while A takes on wider-ranging values. At temperatures well below $\hbar\omega_m/k$, β is essentially independent of T, while at high temperatures $\beta \propto T^{x}$ where the value of x increases with increasing frequency. A number of different theoretical approaches have been proposed to explain these features.[4-12]

A detailed understanding of the temperature dependence is crucial, for it is believed that extrinsic absorption will have a weaker temperature dependence, and thus one could in principle use this to determine whether or not the absorption is intrinsic or extrinsic. In fact, one can show that the absorption due to an nth order process goes as T^{n-1} at high temperat when the "temperature dependence of the phonon freque..ies" is neglected. However, the distinction is not as clear cut as originally proposed because (1) dispersion effects do not allow an immediate determination of the order of the dominant processes from the frequency alone, and (2) the correction due to temperature dependent frequencies can be substantial.

Many of the qualitative features of the frequency and temperature dependence of β described above can be understood using an independent Morse oscillator picture of the

solid.[5,8,11,12] The Morse potential[13]

$$V(r) = D(1 - e^{-\alpha(r-r_o)}) \tag{2}$$

has energy levels

$$E_n = \hbar\omega\,(n + 1/2)\,(1 - \frac{\hbar\omega}{4D}\,(n + 1/2)), \tag{3}$$

$$n = 0, 1, \ldots, \frac{2D}{\hbar\omega} \quad .$$

The parameter, α, is given in terms of the dissociation energy, D, the harmonic frequency, ω, and the reduced mass, μ, by

$$\alpha = \omega\,(\frac{\mu}{2D})^{1/2} \quad . \tag{4}$$

As $D \to \infty$, keeping ω fixed, V(r) becomes a parabola and the second term in Eq. (3) goes to zero. Thus the parameter $\hbar\omega/4D$ may be considered as a measure of the amount of anharmonicity present.

The absorption coefficient for a gas of diatomic molecules is given by

$$\beta = \frac{4\pi^2\rho e^2\Omega}{3\hbar c\, n_o \tilde{Z}} \sum_m \sum_{n>0} \langle m+n|r|n\rangle^2 \tag{5}$$

$$x(e^{-E_m/kT} - e^{-E_{m+n}/kT})\,\delta(\omega_{m+n} - \omega_n - \Omega)$$

where for the Morse potential the matrix elements are approximately

$$\langle m+n|r|n\rangle^2 \simeq \frac{(m+1)(m+2)\cdots(m+n)}{n!} \quad \frac{\hbar}{2\mu\omega} \quad \left(\frac{\hbar\omega}{4D}\right)^{n-1} \qquad (6)$$

for low lying levels. In Eq. (5) ρ is the molecule density, e is the ionic charge, n_o is the index of refraction, and Z is the partition function.

For low temperatures ($T \ll \hbar\omega/k$) only transitions from the ground state will contribute to β, which yields a sequence of delta function lines, one line for each order, n, with their intensities going as $(\hbar\omega/4D)^{n-1}$ (see Eq. (6)). This dependence of β on the order of the transition is analogous to the empirical law (Eq. (1)). For higher temperatures the nth order absorption will contain additional lines due to transitions from higher levels. These lines will be shifted to lower frequencies due to Eq. (3), which provides a basis for the theoretical concept of thermal broadening. Experimentally the multiphonon spectrum is remarkably free of structure even at low temperatures.

It is interesting to note that if one relaxes the infinite lifetime description, the customary Lorentzian line shape cannot be used in place of the delta function because it decays much too slowly. For example, using realistic values for the line width and oscillator strength[14] the calculated absorption in NaCl at 10.6μ due to the fundamental line (assuming Lorentzian line shape) is ~ 10000 times greater than the measured value. The Lorentzian is obtained not only as the solution of the damped oscillator equation (phenomological approach; see ref. 14) but has seemingly more fundamental roots as well.[15] In the latter work the key assumption appears to be that the decay of an excited state of a system goes as $e^{-\lambda t}$. Including life-

time effects in a realistic way is a difficult problem which is avoided by using the delta function description and assuming that the correct line shape decays faster than the matrix elements.

The T^{n-1} law may be obtained by summing over m in Eq. (5) with the assumption that the energy levels are given by their harmonic values. Including the level shifts causes a weaker temperature dependence because energy conserving transitions in the upper levels are necessarily of higher order and therefore less probable.

The main virtue of the Morse potential is that it provides a convenient formalism for including the anharmonicity. Once the anharmonicity parameter is determined the deviation of energy levels from their harmonic values is included implicitly through Eq. (3). By contrast, perturbation treatments include this in an ad hoc way using the distasteful concept of a temperature dependent density of states, when actually, only population factors (not energy levels) depend on temperature.

The main difficulty with the Morse potential treatment, or any independent oscillator approach for that matter, is the obvious one of adapting the formalism to quantitatively describe β for the solid. The possibilities can take on several levels of sopistication relating to the way in which the harmonic frequency is determined. The simplest is the single oscillator picture (just discussed) in which ω is the reststrahl frequency. The dissociation energy may be obtained by fitting to the value of B (Eq. (1)) at room temperature. As we have seen this alone provides a qualitative explanation of the essential features of multiphonon absorption at high temperatures. An improvement is obtained by choosing a distribution of frequencies given by the one phonon density of states of the solid, and integrating Eq. (5) over this distribu-

tion. We have applied this approach using a Debye and more realistic distributions to determine the frequency and temperature dependence of β in alkali halides. Some of these results are presented and discussed below. Those obtained using the Debye distribution have already been reported.[5] A yet higher level of sophistication is attained by integrating first order transitions over the one-phonon density of states, second-order transitions over the two-phonon density of states, etc. The rational for doing this may be better understood by beginning with a realistic model of the solid. From this point of view the Morse potential is used merely as a convenient form for including the anharmonicity. The essential approximation is that the probability of an n phonon transition, goes as (see Eq. (6))

$$W_n \sim \frac{(m+1)\cdots(m+n)}{n!} \quad \frac{\hbar}{2\mu \frac{\Omega}{n}} \quad \left(\frac{\hbar\frac{\Omega}{n}}{4D}\right)^{n-1} \quad \rho_n(\Omega) \qquad (7)$$

where ρ_n is a suitably normalized n phonon density of states. Calculations using this latter approach are presently underway.

At each of these levels finite lifetime effects may be included in an ad hoc way by using a "broadened" density of states. For example, Fig. 1 shows a histogram density of states for KCl[16] along with the broadened density of states. The latter is a sum of Gaussians, one for each step in the histogram, with each having a 20% half width and an area to match that of the histogram. The effect of using the broadened density of states (Fig. 2) is rather dramatic in that it removes the undesired structure with little other effect. The value D = 12000 wavenumbers (cm^{-1}), used in these calculations was chosen from the results in ref. 1 to give the correct slope (B of Eq. (1)) of log β vs frequency (Fig. 3). The

coefficient (A of Eq. (1)) was obtained by normalizing the density of states to the oscillator density of the solid. The temperature dependence of β for KCl at 10.6μ is compared with experiment[17] in Fig. (4). Similar results were obtained for NaCl and NaF but with somewhat poorer agreement. For NaF theory had $\beta \sim T^{1.35}$ at 10.6μ while the measured dependence is $T^{1.7}$.

This kind of agreement is remarkably good, but on the other hand, the ad hoc way in which we removed the structure (Fig. 2) is certainly not very satisfactory. Thus rather than continuing this calculational approach for other materials we are presently pursuing the approach discussed above involving integrations over the n phonon densities of states.

REFERENCES

1. Deutsch. T.F. (1974) J. Phys. Chem. Sol. 34, 2091.
2. Harrington, J.A., and Hass, M. (1973) Phys. Rev. Lett. 31, 710.
3. Pohl, D.W., and Meier, P.F. (1974) Phys. Rev. Lett. 32, 58.
4. Hardy, J.R., and Agrawal, B.S. (1973) Appl. Phys. Lett. 22, 236.
5. Rosenstock, H.B. (1974) Phys. Rev. B 9, 1963
6. Sham, L.J.,and Sparks, M. (1974) Phys. Rev. B. 9, 827.
7. Sparks, M., and Sham, L.J. (1974) Phys. Rev. Lett. 31, 714.
8. McGill, T.C., Hellwarth, R.W., Mangir, M., and Winston, H.V. (1973) J. Phys. Chem. Sol. 34, 2105.
9. Bendow, B., Ying, S.C., and Yukon, S.P. (1973) Phys. Rev. B. 8, 1679.
10. Bendow, B. (1973) Appl. Phys. Lett. 23 133.
11. Mills, D., and Maradudin, A.A. (1973) Phys. Rev. B. 8, 1617.
12. Maradudin, A.A., and Mills, D. (1973) Phys. Rev. Lett. 31, 718.
13. See ref. 5 for a detailed review of the quantum mechanics of the Morse potential.
14. Born, M., and Huang, K. (1954) Dynamical Theory of Crystal Lattices (Oxford U.P., London).
15. Weisskopf, V., and Wigner, E. (1930) Zs. f. Phys. 63, 54. (See W. Heitler, Quantum Theory of Radiation (Oxford U.P., London 1954) p. 181-189.
16. Raunio, G., and Rolandson, S. (1970) Phys. Rev. B. 2, 2093.
17. (1973) Semi-Annual Report No. 3, ARPA Order 2031, Naval Research Laboratory, 46.

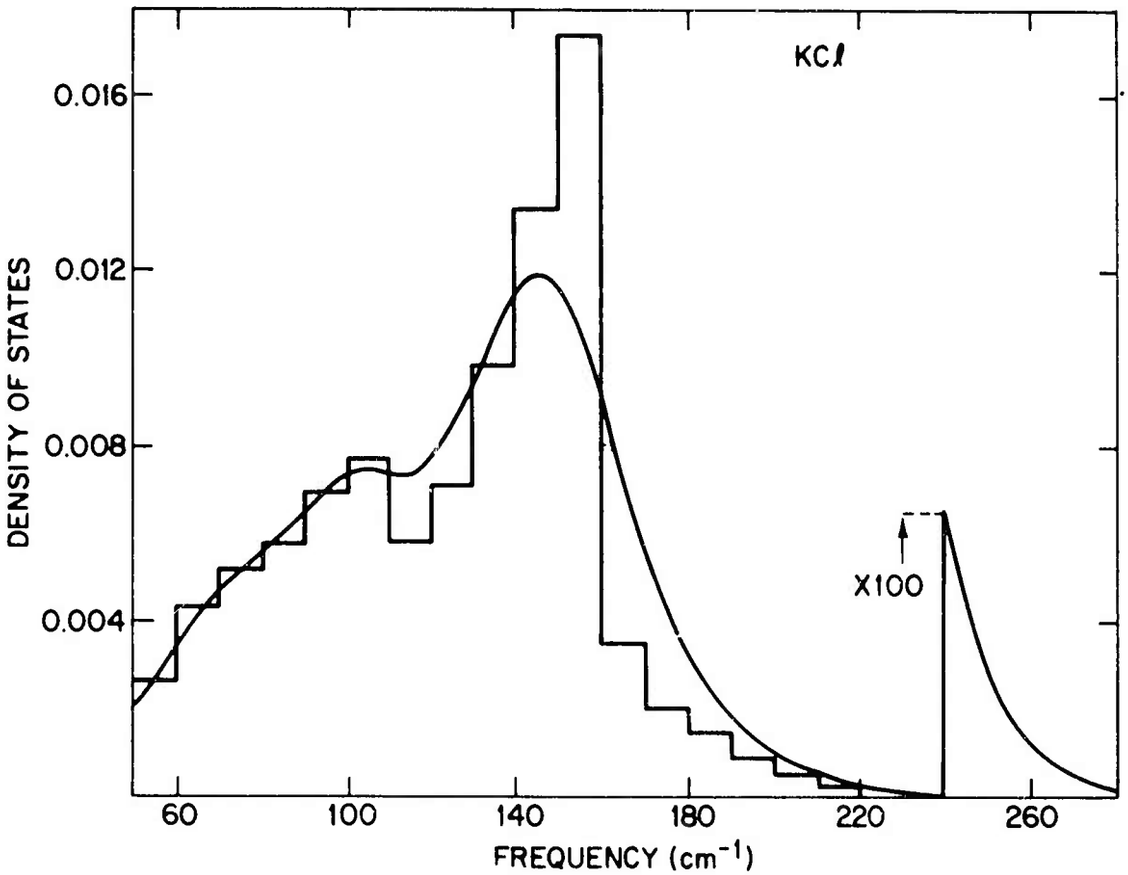

1. Density of states for KCl (histogram, taken from ref. 16) along with a "broadened" density of states (smooth curve).

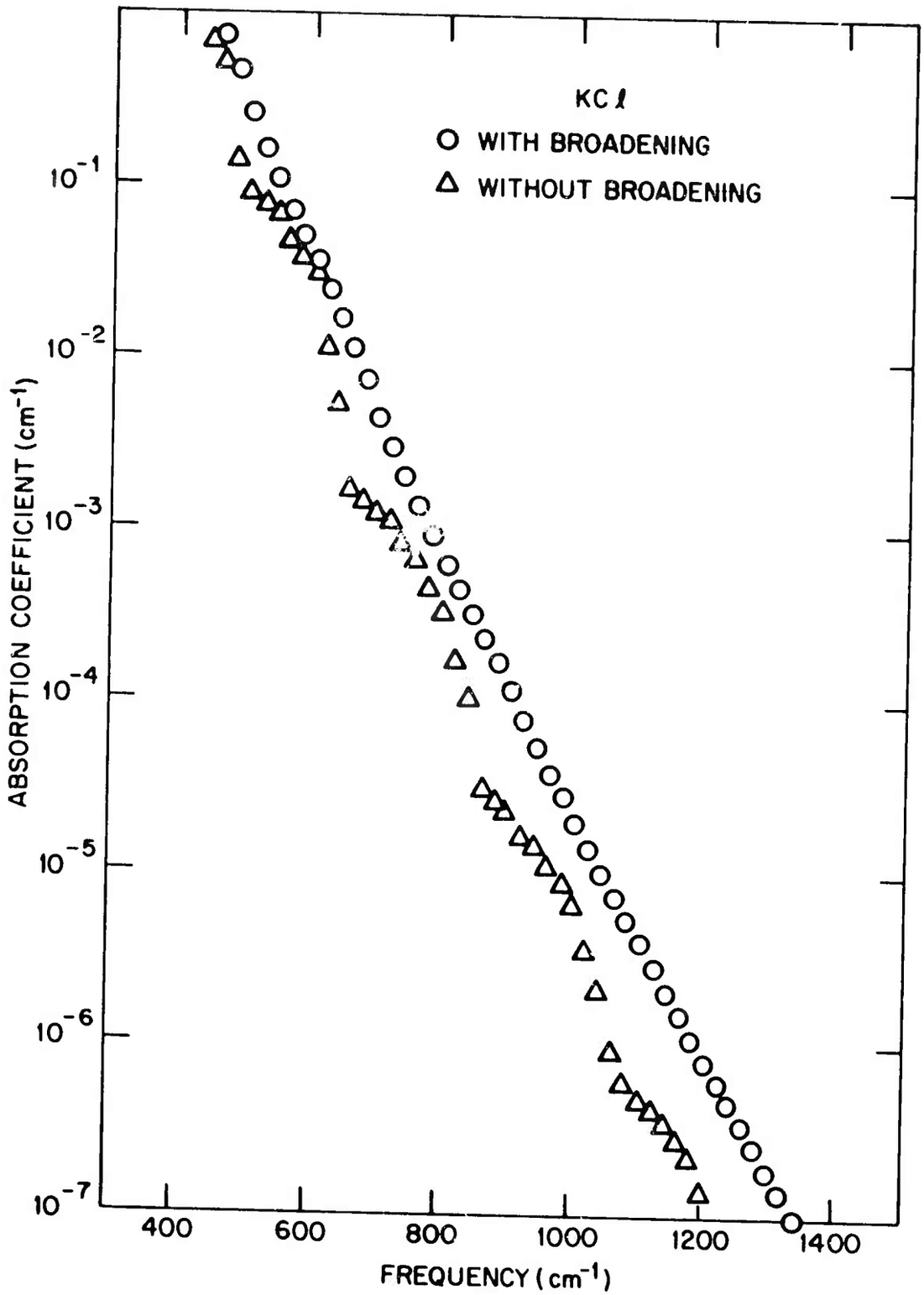

2. Calculated room temperature absorption coefficient as a function of frequency using the histogram and the broadened density of states shown in Fig. 1.

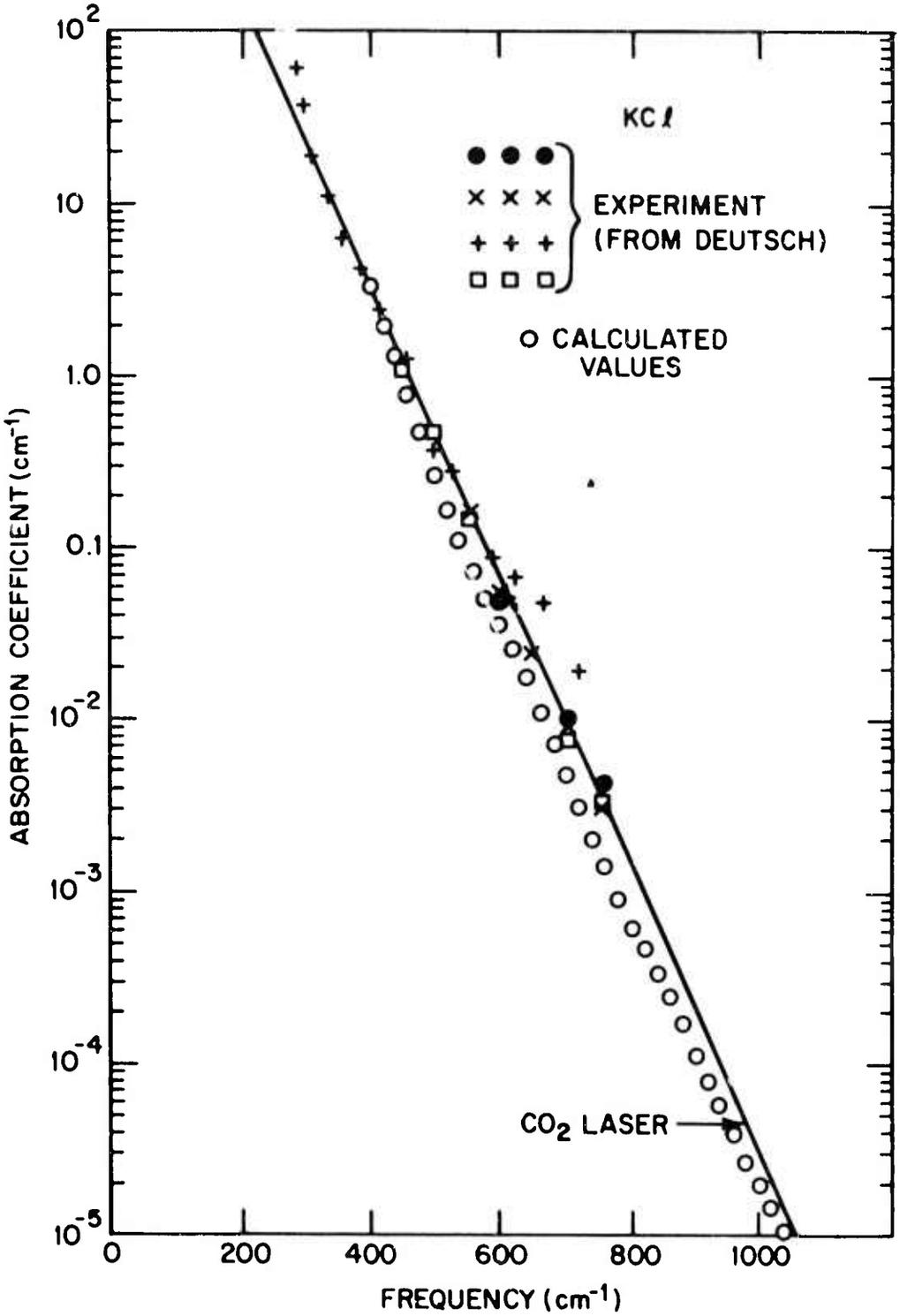

3. Comparison of the theoretical and experimental frequency dependence of the room temperature absorption coefficient of KCl. Experimental results are from ref. 1.

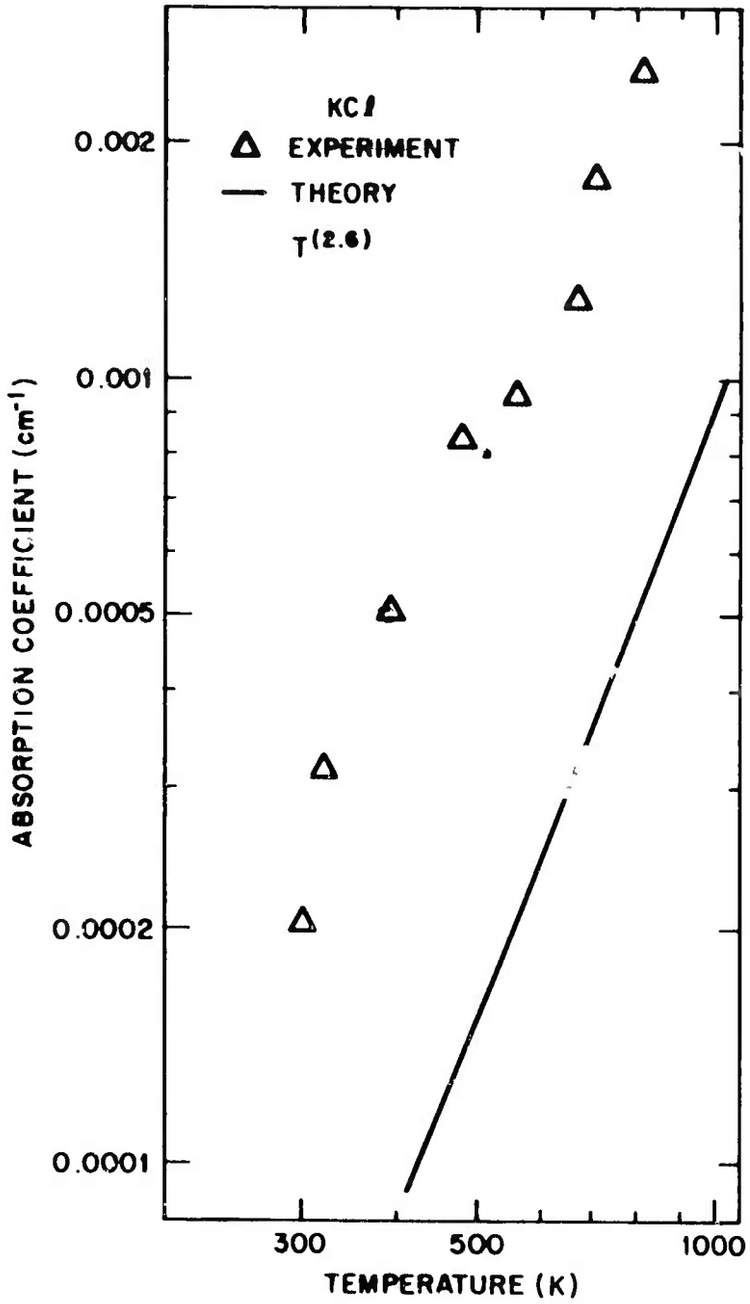

4. Comparison of the theoretical and experimental temperature dependence of the absorption coefficient of KCl at 10.6μ. Experimental results are from ref. 17.

IMPURITY EFFECTS ON VACUUM ULTRAVIOLET AND INFRARED MULTIPHONON SPECTRA OF LASER-WINDOW MATERIALS

PHILIPP H. KLEIN, M. KRULFELD,
and ESTHER W. CLAFFY
U.S. Naval Research Laboratory
Washington, D.C. 20375

Abstract

Vacuum-ultraviolet (VUV) absorption spectra of the surfaces of KCl crystals show them to be sensitive to exposure to the atmosphere. Surface absorption in the 185-195 nm region increases more than fivefold during a four-hour exposure in the laboratory. In the less-soluble NaF, VUV surface absorption is virtually unchanged after days of exposure to air, although the initial absorption is much greater than is the case in KCl. In NaF, a potential window material in the 2-6 μm region, IR absorption throughout the multiphonon region is the smallest reported for that material to date. Intrinsic behavior appears to have been attained in this region, although prior work also has shown the appearance of "intrinsic" behavior. Contamination by OH^- can be excluded as a cause of these observations, although cause by another unidentified contaminant cannot be ruled out.

1. INTRODUCTION

Attainment of intrinsic absorption in window materials is an implicit goal of the laser window program. Intrinsic absorption in the infrared (IR) region of the spectrum is generally recognized by an exponential decrease in absorption with increasing frequency. Failure to observe this decrease may be due to several factors, of which presence of optically-absorbing impurities within the bulk of the crystal or at its surface is the main concern here.

Divalent dopants (e.g., Sr^{+2}, Ba^{+2}), added to increase the strength of potassium chloride, do not directly affect the absorption at the IR wavelengths of interest. On the other hand, presence of oxygen-containing anions (e.g., OH^{-}, CO_3^{--}, or ClO_3^{-}) has been shown (1) to be associated with increased IR absorption. Surface contamination by these anions during exposure of KCl crystals to the atmosphere is suggested by infrared emissivity measurements (2). Results of spectrophotometric measurements in the vacuum-ultraviolet (VUV) region of the spectru, confirming the sensitivity of KCl surfaces to atmospheric exposure, are reported in this section.

In contrast with the relatively large exposure-induced changes in surface absorption found in KCl crystals, VUV measurements on sodium fluoride crystals show no perceptible change even after the specimen has stood for days in air. This observation suggests ease of handling of this potential window material for the 2-6 μm region.

More important, measurements are presented here which show that NaF crystals, as prepared in our laboratory, exhibit intrinsic IR absorption. The parameters of the observed exponential decrease in absorption with increasing frequency differ from those given in previous work dealing

with what was thought to be intrinsic absorption in NaF (3-5). The present, unexpected result suggests that re-examination may be warranted of multiphonon exponential absorption in other materials whose purity has been substantially increased.

2. EXPERIMENTAL

The potassium chloride crystal used in this study had a measured absorption coefficient of 0.0002 cm^{-1} at 10.6 micrometers. It was grown in our laboratory by the Bridgman process, under an atmosphere of carbon tetrachloride carried in titanium-gettered argon. A piece, measuring 0.447 X 0.836 X 1.331 cm was cleaved from this crystal (No. B221), polished in concentrated hydrochloric acid, wiped dry, and immediately placed within the vacuum chamber of the spectrophotometer. An adjacent portion of crystal No. B221, 0.372 cm thick, was used for atmosphere-exposure studies.

Three different sodium fluoride crystals were used. All were grown by the Czochralski method in our laboratory, using the purification technique evolved here (6). The method involves recrystallization of sodium hydrofluoride ($NaHF_2$) from hydrofluoric acid, regeneration of NaF by heating $NaHF_2$ in titanium-gettered argon, and pulling of a crystal, also under purified argon. Crystals were wire-sawn to approximate size (cleaving is difficult in pure NaF), using diamond-impregnated wire and isopropanol as the lubricant. Surfaces which were to transmit light were polished with Linde A alumina, carried in fresh isopropanol. Crystal No. 98X, measuring 0.740 X 0.929 X 1.681 cm, was used for VUV measurements. Crystal No. 49G, 4.10 cm long, and Crystal No. 39, 8.25 cm long, were used for differential IR spectrophotometry.

Vacuum ultraviolet measurements were made with a McPherson Model 225 double-beam spectrophotometer, using a hydrogen-lamp source and vacuum as reference. For KCl, data were taken over the range from 180 nm to 220 nm. Sodium fluoride data covered the range from 130 nm to 170 nm. Infrared measurements were made with a Perkin-Elmer Model 521 double-beam spectrophotometer. Differential data were taken throughout the range from 2.5 μm to 12 μm (approximately 4000-700 cm^{-1}).

Correction for reflection losses was made for VUV data, using data of Smakula (7) for KCl and those of Tomiki and Miyata (8) for NaF. No reflection corrections were necessary for the differential infrared spectra. Instrumental corrections were made for all data.

3. RESULTS AND DISCUSSION

A. KCl

The bulk absorption coefficient, defined in Eq. (1), may be used for calculating the OH^- content of Crystal No. B221:

$$\beta_T{}^{\ell} = \beta_s + \beta\ell \qquad (1)$$

Here, β_T is the total absorption coefficient, ℓ is the length, β_s is the surface absorption, and β is the bulk absorption coefficient. Equation (1) is the basis for using $\beta_T{}^{\ell}$-vs-ℓ plots to determine β_s and β.

The conversion factor for OH^- content is 2.4 mol ppm/cm^{-1}, where the absorption coefficient is determined at 205 nm (9). From the measured value of β at 205 nm (0.052 cm^{-1}), the bulk OH^- concentration is 0.12 mol ppm. The low value attests to the efficacy of heating in carbon tetrachloride vapors for removal of OH^- from KCl.

Exposure-induced changes in total absorption coefficient and in surface absorption are greatest, according to Figs. 1 and 2, in the 185-195 nm region, away from the OH^- absorption band at 205 nm. This makes it clear that simple hydrolysis of KCl is not responsible for the increased absorption, and that some other ion (e.g., HCO_3^- or ClO_3^-) may likely be involved. Present data do not permit pinpointing the identity of the absorbing species, but it is noteworthy that similar conclusions have been drawn from IR absorption data (1).

B. NaF - VUV Data

One might expect lessened sensitivity to atmospheric moisture in NaF, since it is only about one-eighth as soluble in water as is KCl. Not only does NaF show little tendency to change its VUV absorption characteristics on standing in air, but, as shown in Fig. 3, its surface absorption has a structureless variation with wavelength. Considering the magnitude of the surface absorption measured directly after polishing, it may be that damage during polishing is sufficient to mask further surface deterioration resulting from hydrolysis.

The peak at 151 nm in the total-absorption-coefficient curve of Fig. 3 corresponds exactly to the accepted wavelength (10) of the OH^- absorption in NaF. The concentration of OH^- required to produce this peak is about 1.1 mol ppm (0.7 mol ppm/cm^{-1} (10)). This is a reasonable value for Crystal No. 98, which was only grown once. Crystals Nos. 39 and 49 were both grown from material which had itself been grown into a crystal after purification, hence can be expected to be freer of hydroxyl contamination.

C. NaF - IR Data

In the multiphonon region involving three to five phonons, the logarithms of the absorption coefficients

of most pure alkali halides fall on straight lines with negative slopes, when they are plotted as functions of frequency. The appearance of such a curve is normally taken as evidence that intrinsic behavior has been attained.

At least three distinct straight lines can be passed through the sets of data plotted in Fig. 4. It is noteworthy that the slopes of the curves increase with the modernity of the data, from 1937 (3) through 1958 (4) to 1974 (11). It is also worthy of note that the data of McNelly and Pohl (11) agree most closely with the present results. In addition, it can be seen that the smallest absorption coefficients reported are these latest data. Such observations suggest that improvements in purification and growth methods have eliminated some impurity.

The possibility of an impurity absorption being responsible for the changes shown in Fig. 4 gains credibility from the recent observation (5) that NaF crystals grown in air had greater absorption at 10.6 μm than did those grown in argon. It is possible that an impurity analogous to that producing absorption in alkali chlorides in the 10-μm region (1) is responsible for the absorption seen here in NaF.

The historical changes in the IR absorption spectrum of NaF show that impurity effects not associated with discrete absorption bands may be present even when the data strongly suggest "intrinsic" behavior. Evidently, experimental indications of intrinsic multiphonon absorption cannot be relied upon with certainty.

4. CONCLUSIONS

Exposure of KCl to laboratory air produces changes in its absorption spectrum which cannot be attributed to simple hydrolysis and consequent introduction of OH^- ions

into the surface. Similar exposure of NaF crystals does not result in analogous changes in surface absorption, although surface damage during polishing may mask some subtle effect.

Present results are the smallest infrared absorption coefficients ever reported for NaF, and correspond to intrinsic behavior. No immediate explanation can be found for there having been two previous observations of "intrinsic" absorption, but with larger absorption coefficients. While it is unlikely that OH^- contamination is responsible for these observations, the possibility that a single absorbing impurity is responsible for both the chloride and the fluoride observations cannot be ruled out.

ACKNOWLEDGEMENTS

It is a pleasure to acknowledge fruitful discussions with Dr. M. Hass of this laboratory and with Prof. N. Bloembergen, of Harvard University. The experimental guidance in VUV measurements afforded by Drs. G.H. Sigel, Jr. and B.D. Evans is also gratefully acknowledged.

1. Lipson, H.G., Larkin, J.J., and Bendow, B., "Impurity Absorption in KCl Windows", from Third Conference on High-Power Infrared Laser Window Materials, AFCRL-TR-74 -008(I), 14 February 1974, edited by C.A. Pitha and B. Bendow, p. 236.

2. Hass, M., and Stierwalt, D.L., "Spectral Emittance Studies of Surface and Bulk Absorption", from High Energy Laser Windows: Semi-Annual Report No. 4, ARPA Order 2031, Naval Research Laboratory, 30 June 1974.

3. Hohls, H.W., "Dispersion und Absorption von Lithium-fluorid und Natriumfluorid", Ann. Physik 29, 433 (1937).

4. Klier, M., "Die Temperaturabhaengigkeit der optischen Konstanten von Lithiumfluorid und Natriumfluorid im Ultraroten", Z. Physik 150, 49 (1958).

5. Pohl, D.W., and Meier, P.F., "Multiphonon Absorption in NaF", Phys. Rev. Letters 32, 58 (14 January 1974).

6. Collins, W.C., Schneider, I., Klein, P.H., and Johnson, L.R., "Additive and Electrolytic Coloration of NaF", Appl. Phys. Letters 24, 403 (1 May 1974).

7. Smakula, A., "Einkristalle: Wachstum, Herstellung, und Anwendung", Springer Verlag, Berlin, 1962, p. 386.

8. Tomiki, T., Miyata, T., "Optical Studies of Alkali Fluorides and Alkaline Earth Fluorides in VUV Region", J. Phys. Soc. Japan 27, 658 (1969).

9. Klein, M.V., Kennedy, S.O., Gie, T.I., Wedding, B., "The Hydroxyl Ions in Alkali Halide Crystals - Crystal Growth and Characterization", Mat. Res. Bull. 3, 677 (1968).

10. Meistrich, M.L., "U.V. and I.R. Absorption in OH^- -Doped NaF", J. Phys. Chem. Solids 29, 1119 (1968).

11. McNelly, T.F., and Pohl, D.W., "Multiphonon Optical Spectrum of NaF", Phys. Rev. Letters 32, 1305 (10 June 1974).

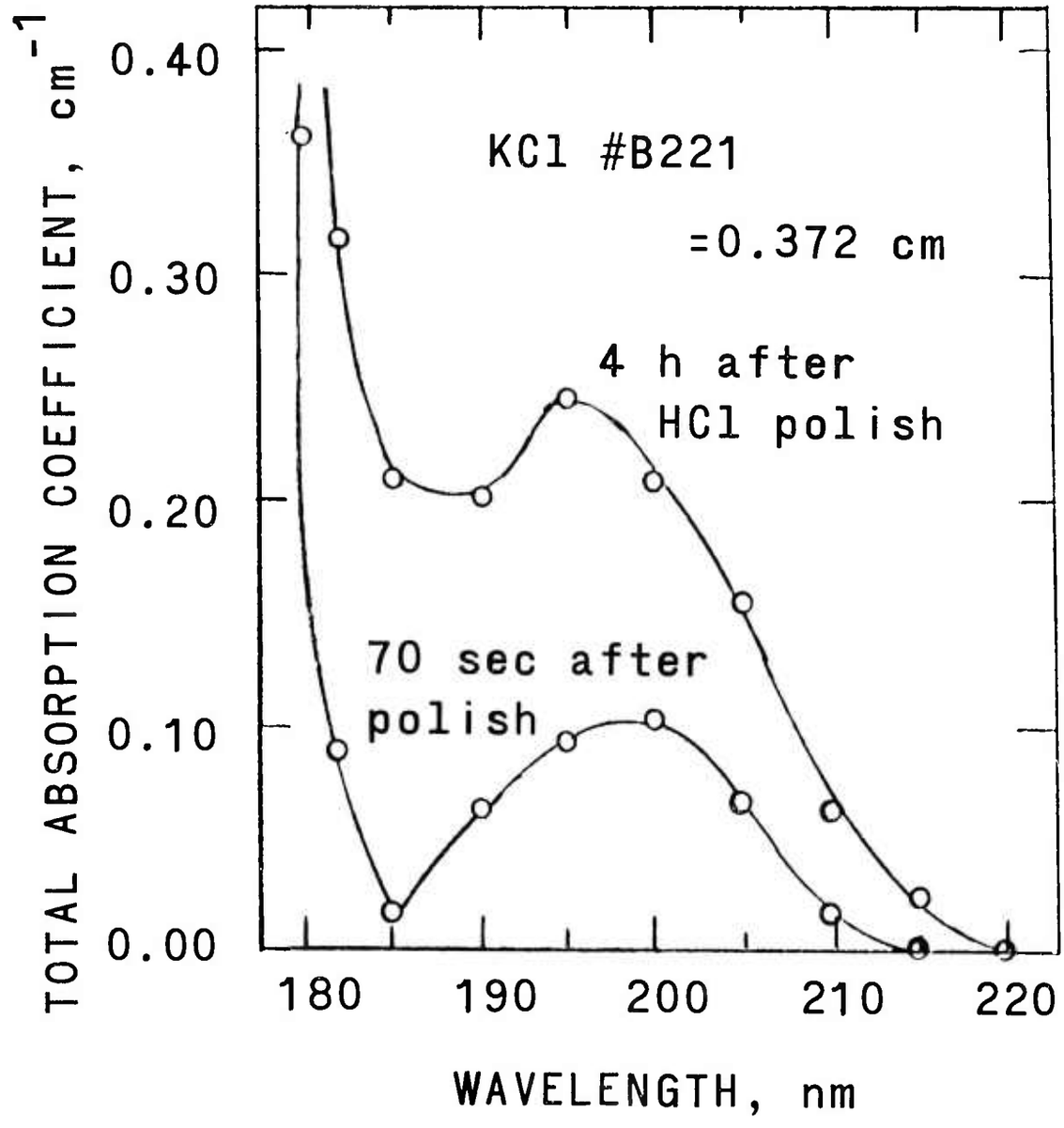

Fig. 1. Vacuum ultraviolet absorption coefficient of KCl Crystal No. B221. Lower curve: 70 seconds after removal from HCl polishing solution. Upper curve: after four hours of exposure to laboratory air.

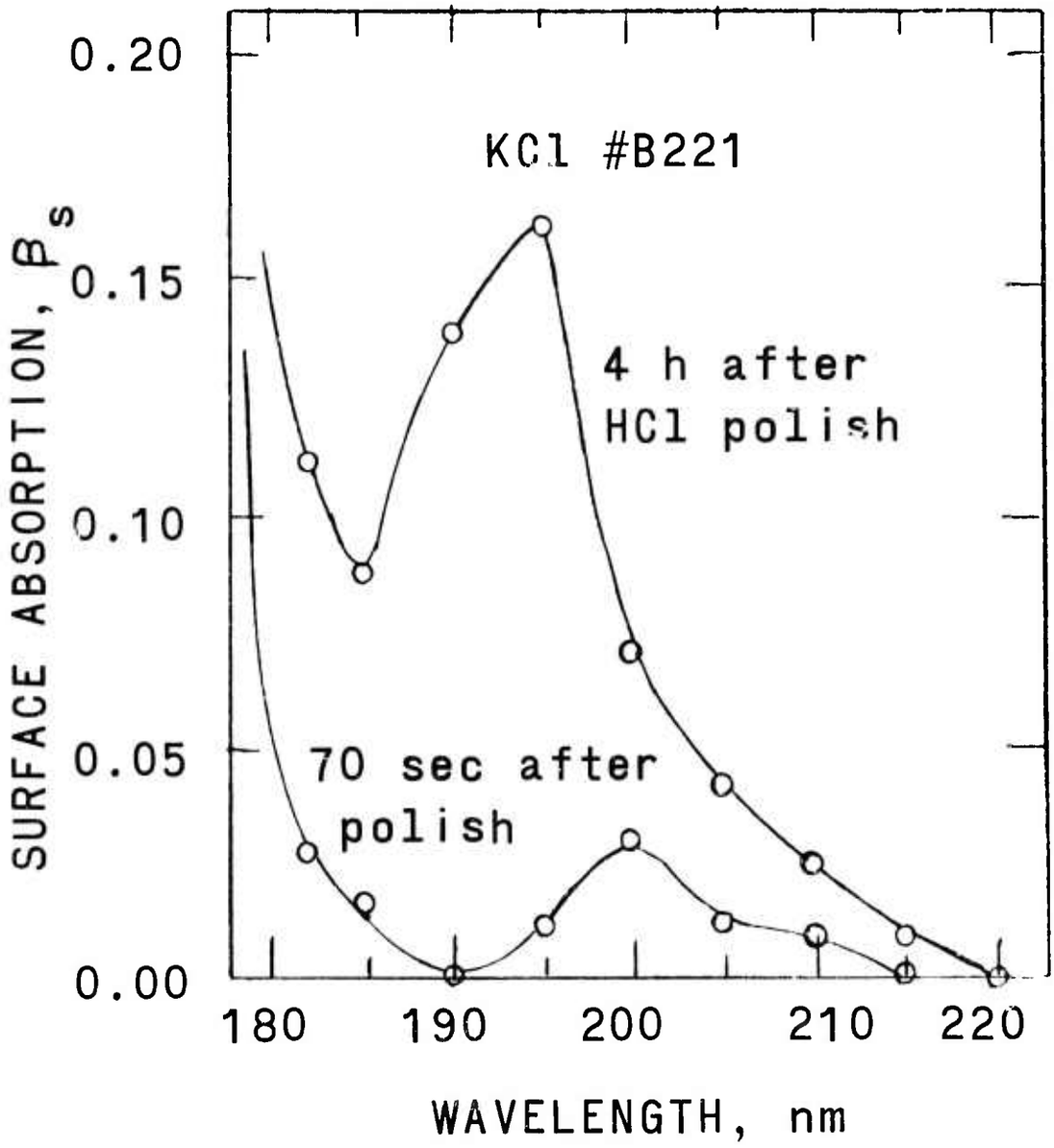

Fig. 2. Surface absorption of the KCl crystal of Fig. 1. It is significant that the OH^- absorption band at 205 nm is only slightly affected by air exposure.

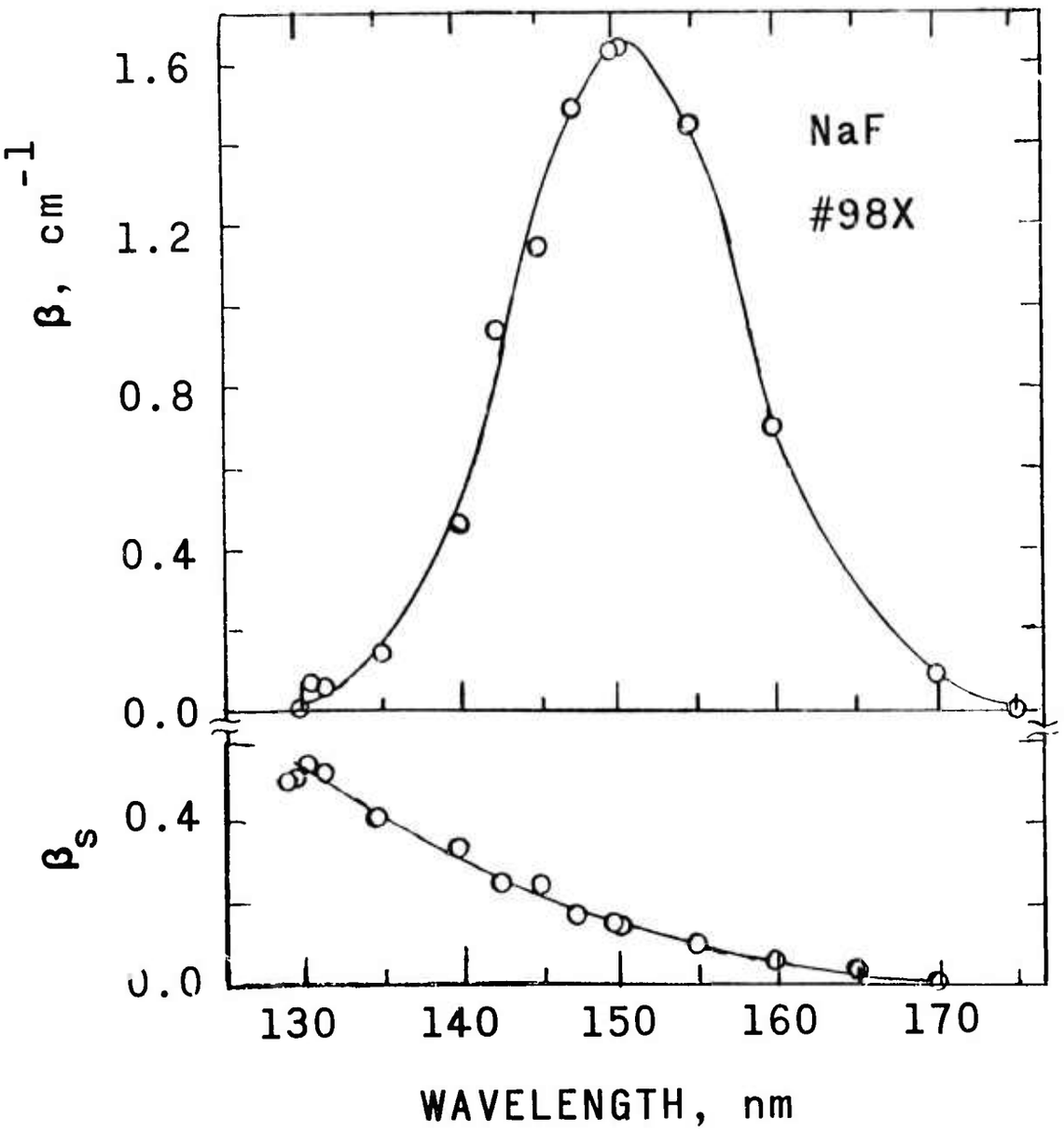

Fig. 3. Vacuum ultraviolet absorption coefficient (upper graph) and surface absorption (lower graph) of NaF Crystal No. 98 X. Curves were unchanged after several days' exposure of the crystal to the air.

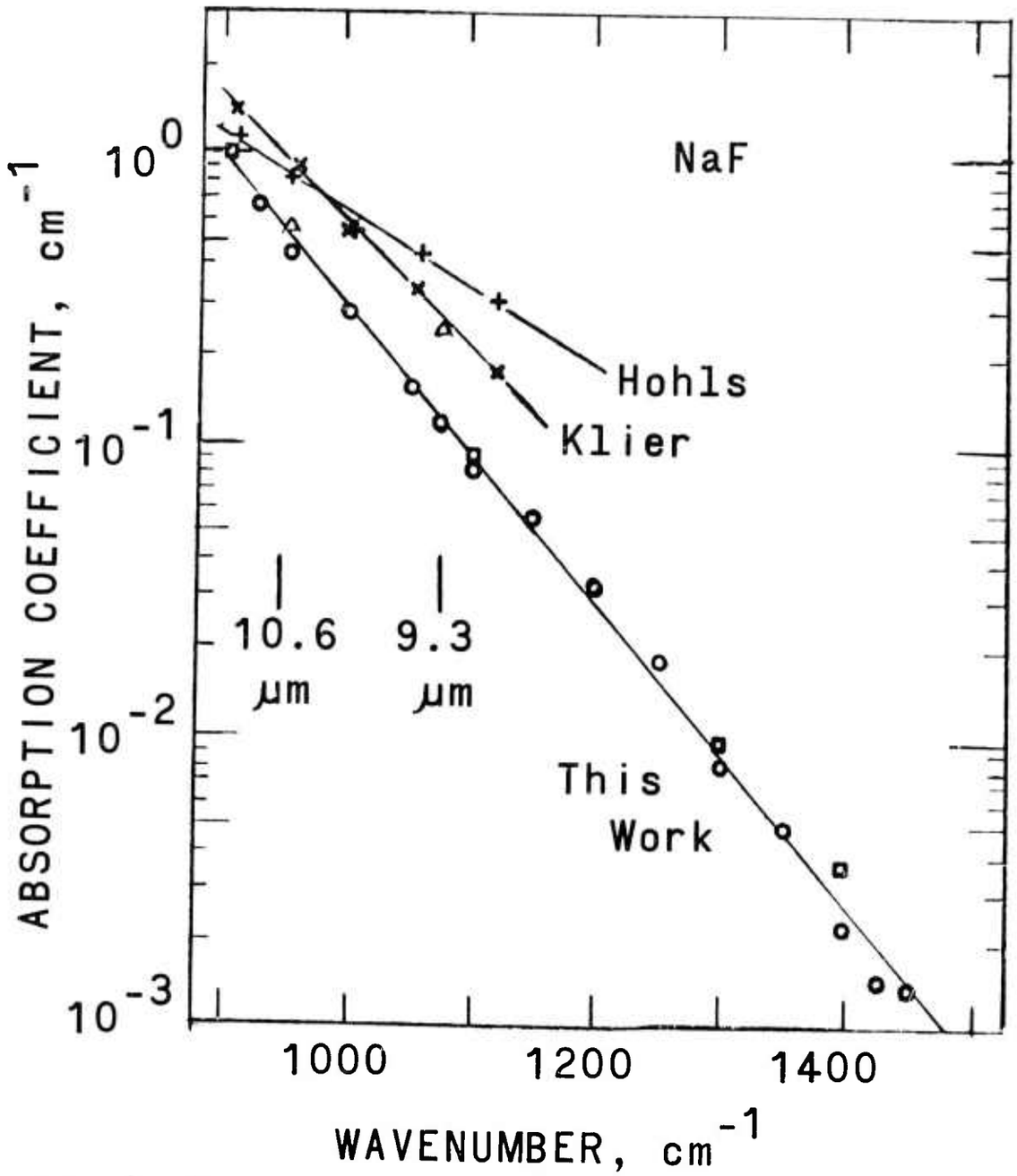

Fig. 4. Absorption coefficient of NaF in the infrared. Present results (circles) were obtained by differential measurements (Crystals Nos. 39 and 49G), using a pathlength difference of 4.15 cm. Data of Ref. 3 are shown as +, those of Ref. 4 as crosses, and those of Ref. 11 as squares. The two triangles, from recent data of Ref. 5, lie on a line roughly parallel to the early data of Hohls.

SURFACE FINISHING OF FLUORIDE LASER WINDOWS

J.W. Davisson
Naval Research Laboratory
Washington, D.C. 20375

Abstract

Previous work at this Laboratory has shown that scratch-free high quality surfaces can be easily produced on the alkali chlorides by controlled chemical polishing.[1,2] In this reporting period, some attempts were made to employ this approach for fluoride laser windows. Currently, fluoride laser windows can be mechanically polished by conventional or bowl-feed techniques to finishes of high quality. Chemical polishing holds the promise of further improvement and might provide easy surface preparation for examination of specimens for optical absorption studies. The preliminary results given here indicate that best results can be obtained for NaF and fair results for the alkaline earth fluorides. However, the dramatic results obtained for the alkali chlorides could not be obtained for the fluorides and in fact might not be necessary. However, all of the surface problems with fluorides laser windows are not completely known as there are some indications that some surface treatment or surface passivication may be desirable for reliable operation in a fluoride gas atmosphere.

The alkali and alkaline fluorides were found to be less amenable to chemical processing techniques than the alkali chlorides. This difference may be due to the lower solubility and the higher lattice energy of the fluorides. The lower solubility precludes the use of chemical processing techniques for rapid cutting and grinding operations and thus restricts the chemical processing to surface finishing. Here chemical polishing was achieved on LiF and NaF crystals by means of a generalized surface dissolution mechanism rather than by the uniform migration of steps. As a consequence these polished surfaces show a granular texture instead of the microscopically smooth surfaces obtained on the alkali chlorides. The elimination of etch pits by means of chemical action was difficult to achieve in the alkaline fluoride crystals CaF_2 and BaF_2 probably because the influence of dislocations, especially with regard to the chemical potential at the surface, becomes more pronounced as the lattice energy is increased. Therefore the solvents employed can only be used as pseudo-chemical polishes to soften surface scratches before dislocation etch pits have formed. The detailed observations dealing with the chemical polishing with various fluoride crystals are described below.

LiF

Gilman and Johnston[3] found that a chemical polishing action, characterized by the ability to virtually remove etch pits, was achieved on LiF by violently agitating the crystal in a weak ammonia solution. Since the surfaces obtained by this method (Fig. 1) show a granular texture, a generalized surface dissolution mechanism rather than the uniform migration of steps probably dominates the action. By suitable refinement of technique a much finer texture than that shown in Fig. 1 can undoubtedly be obtained, but the achievement of a microscopically smooth surface seems unlikely.

NaF

Since the surface of the NaF crystal appears to be unstable in water and in aqueous solutions of HF as shown in Fig. 2, the addition of a metallic poison is required to stabilize the dissolution process. Many metallic ions will produce the required stabilization, but they also produce dislocation etch pits. A chemical polish based on the manganous ion[4] will provide a good chemically polished pit-free surface on an annealed single crystal of NaF as shown in Fig. 2. The crystal was annealed at 400°C to relax the stress fields about new edge dislocations to which influence this solution is sensitized. This surface shows a granular texture.

CaF_2 and BaF_2

Harrington[5] has examined the action of sulfuric acid - acetic acid mixtures on the dissolution of CaF_2 and BaF_2 surfaces and has observed the widening of surface scratches and the softening of their sides. Our study of these surfaces confirm his findings. Harrington's acid solutions as well as solutions of other acids appear to be dislocation etchants for the CaF_2 crystal. Thus these solutions can only be used as pseudo-chemical polishes to soften surface scratches before dislocation etch pits have formed. The BaF_2 crystal was found to be slightly soluble in distilled water and in aqueous solutions of acids. Prolonged dissolution produced a deeply pitted surface of random etch pits. Since dislocation etch pits were not identified on the BaF_2 surface, it seems more likely that a good chemical polish can be developed for BaF_2 than for CaF_2 crystals. Examples of the dissolution behavior of these crystals are shown in Figures 3 and 4.

DISCUSSION

The alkali and alkaline fluorides are found to be less amenable to chemical processing techniques than the alkali chlorides. Chemical polishing characterized by the ability to remove etch pits was achieved with the alkali fluorides but not with the alkaline fluorides. The existence of texture in the chemically polished surfaces of LiF and NaF suggests that the mechanism of polishing may be a generalized surface dissolution process rather than a uniform surface migration of steps. Thus microscopically smooth surfaces were not obtained. The elimination of etch pits by means of chemical action was difficult to achieve in the alkaline fluorides.

Since the fluorides are harder than the chlorides, they can be mechanically processed with less damage than the chlorides. In particular the action of scratching by means of mechanical polishing produces little if any dislocation damage in the alkaline fluorides. One can see this from the enlargement in Fig. 3 which shows no evidence of etch pits in the vicinity of the widened scratches. Since no evidence is observed of plastic yielding in the surface, it seems likely that an excellent surface finish can be obtained on alkaline fluoride windows by mechanical means. It remains to be seen whether the transparency or the integrity of such surfaces can be improved by chemical treatments.

1. Davisson, J.W. (1972) "Chemical Polishing of NaCl and KCl Laser Windows" from 1972 Conference on High Power Infrared Laser Window Materials, AFCRL-TR-73-0372 (II) (19 June 1973), edited by C.A. Pitha, p. 525, See also "High Energy Laser Windows", Semiannual Report Nos. 1, 2, and 3 (1973), ARPA Order No. 2031, Naval Research Laboratory. See also Journal of Materials Science (in press).

2. Braunstein, M. (1973) "Laser Window Surface Finishing and Coating Technology", AFCRL-TR-74-0032, Contract F19628-73-C-0243, Project 2415, Semiannual Report 1 (1973). ARPA Order 2415.

3. Gilman, J.J. and Johnston, W.G. (1957) Dislocations and Mechanical Properties of Crystals edited by Fisher et al. John Wiley and Sons, Inc. New York, 1957, p. 121.

4. Davisson, J.W., and Levinson S., J. Appl. Phys. 37, 4888 (1966).

5. Harrington, J., University of Alabama, Huntsville, Alabama 35807, private communication.

Fig. 1. Surface of LiF crystal chemically polished in dilute ammonia solution. Nomarski micrograph (320X).

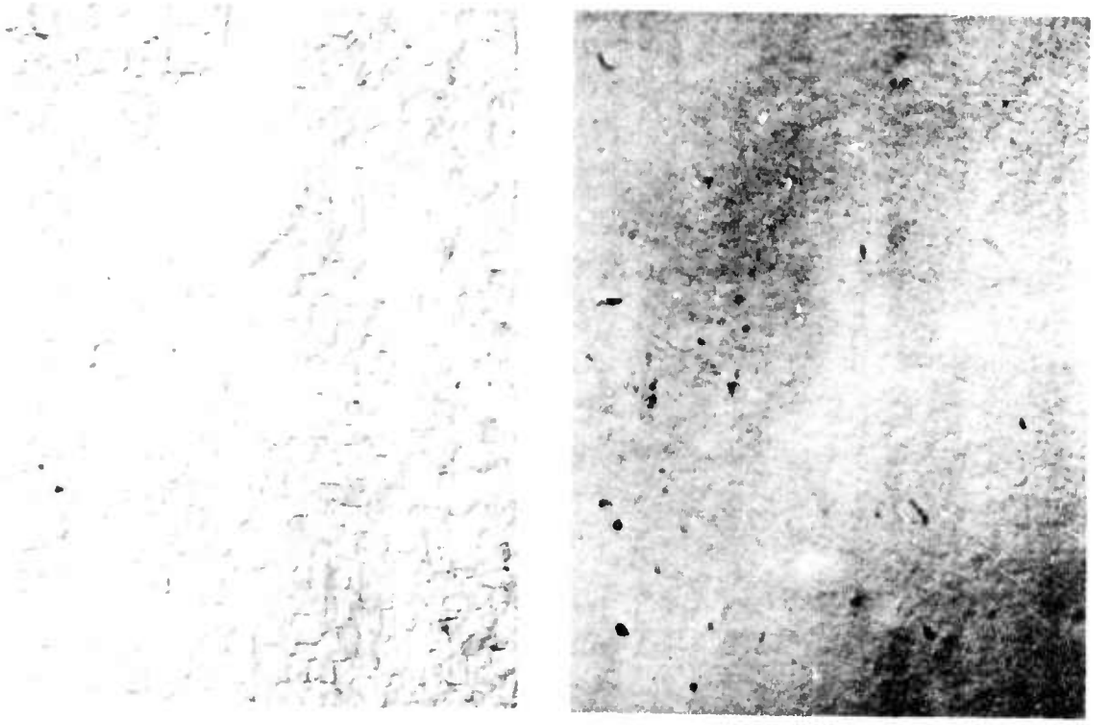

Fig. 2. Surfaces of NaF crystals

Left: Typical texture obtained by dissolution in water and in dilute HF solutions.

Right: Chemically polished in Mn^{++} polishing solution. Nomarski micrographs (320X).

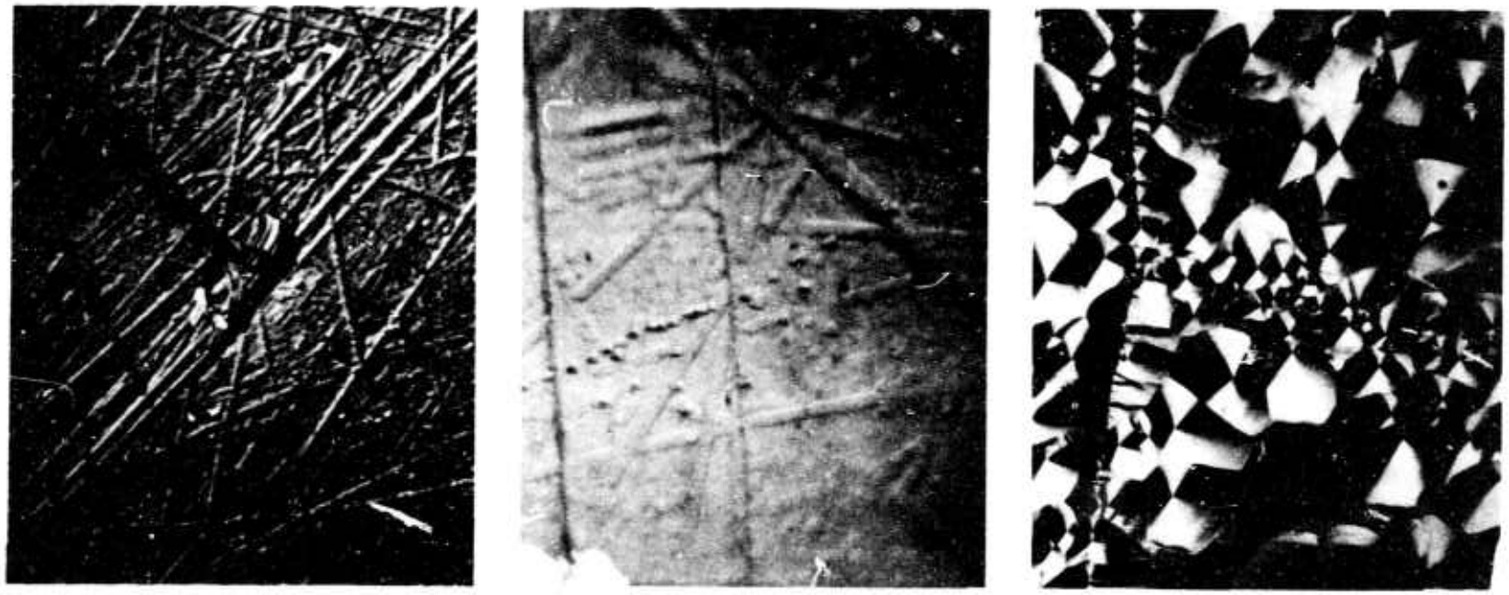

Fig. 3. Chemical action on mechanically polished CaF_2 crystal using Harrington 3/2(H_2SO_4/CH_3COOH) solution.

Left: Surface scratches are broadened and dislocation etch pits are formed after 2 hr. dissolution (320X).

Middle: An enlargement of the scratches (800X) shows smooth pit-free grooves.

Right: Prolonged dissolution (40 hr) produced an etched, deeply pitted surface comprised of dislocation etch pits (320X).

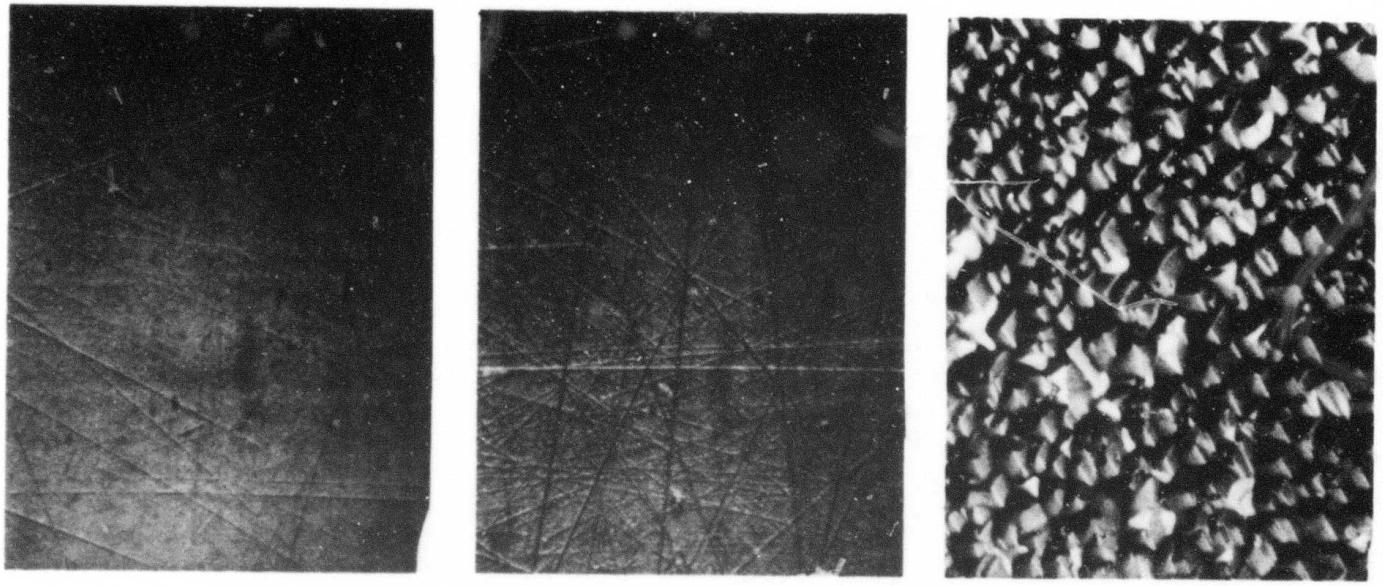

Fig. 4. Chemical action on mechanically polished BaF_2 crystal using distilled water.

Left: Mechanically polished surface.

Middle: Surface scratches are broadened after 2 min. dissolution.

Right: Surface obtained after 12 hr. dissolution Nomarski micrograph (320X).

SPECTRAL EMITTANCE STUDIES OF SURFACE AND BULK ABSORPTION

M. Hass
Naval Research Laboratory
Washington, D.C. 20375

D.L. Stierwalt
Naval Electronics Laboratory
Center, San Diego, CA 92152

1. INTRODUCTION

Spectral emittance studies are particularly important to the laser window program as they provide a measurement of low absorption coefficients over a wide wavelength range. While current instruments are not as sensitive as laser calorimetry, they nevertheless have sufficient sensitivity for many aspects of the window program.

In this report some studies of surface and bulk absorption in laser window materials are reported using the spectral emittance apparatus at the Naval Electronics Laboratory Center, San Diego. They represent a continuation of previous studies carried out by Stierwalt and Harrington. In the previous studies of Harrington and Stierwalt, the spectral emittance of KCl grown in a reactive atmosphere and with surface prepared by chemical polishing were studied. These investigations showed that for the first time that the very low absorption coefficients ($\sim$0.0002 cm^{-1}) observed in the low loss KCl by laser calorimetry were consistent with measurements obtained by spectral emittance. KCl crystals from other sources always appeared to show a definite band at around 9.5 μm. The intensity of this band was greatly reduced for crystals grown in a reactive atmosphere. In addition to KCl, a number of other laser window materials were studied and valuable experience on the use of spectral emissivity for measurement of low absorption coefficients was obtained. Some temperature dependence studies have been reported by Stierwalt at the 1973 Hyannis meeting.[1]

In this present report, an attempt was made to continue studies of the frequency and temperature dependence of intrinsic absorption in order for comparison with a number of theoretical treatments of the subject. While some progress towards this goal was achieved, the accuracy of the results is not sufficiently good at this time for comparison with theory. However, in the course of obtaining these observations, a rather interesting effect pertaining to surface absorption in KCl was noted and studied. In particular, a surface absorption band at around 9.5 μm has been reported in previous work from NRL and other laboratories. While the specific origin of this band is still in question, a technique for largely eliminating the surface absorption band was discovered and is reported here. This discovery is believed to be of great importance for the laser window program.

2. EXPERIMENTAL

The experimental apparatus employed for these investigations has been described previously.[2] The sensitivity of this apparatus is sufficient such that for samples several cm in length, absorption coefficients in the range of 0.0001 cm^{-1} can be measured over a wavelength range of 3-22 μm. However, these numbers are subject to some qualification. When highly transparent materials are studied, there appears to be a zero level correction which can not always be estimated accurately since it is both a function of wavelength and the type of sample being studied. The spectral emittance of the empty sample holder itself can be obtained and this provides some guide as to the zero level. However, this may only be part of the zero correction. Scattering of the radiation emitted by the sample holder by the sample may also contribute to this zero correction.

This zero correction problem is illustrated in Fig. 1 in which the spectral emittance of the sample and of the empty sample holder are shown. At the time this data was taken, the emittance of the empty sample holder was several times larger than has been observed on previous occasions. The emittance with the sample is always larger, but at shorter wavelengths where the intrinsic absorption is effectively zero, the additional emittance might actually arise from scattering rather than a true absorption.

The curves in Fig. 1 gave some idea of the problems involved with the existing system. A great improvement in the signal-to-noise ratio should be obtained with an emittance spectrometer with cooled walls as proposed by Stierwalt. Since the emittance signal depends upon the difference in temperature between the sample and the surrounding container, cooled walls should decrease unwanted radiation of the type manifested in the zero correction. Other improvements should also result from different types of sample holders designed to minimize stray radiation and from polishing techniques minimizing scattering. Success in measuring very low absorption coefficients may not necessarily depend upon the achieving nigh sensitivity and resolution, but rather on eliminating sources of unwanted stray radiation.

3. SPECTRAL EMITTANCE OF 9.5 μm SURFACE ABSORPTION BAND IN KCl

Even in the best KCl crystals which have been grown at NRL and carefully polished, an absorption band of surface origin occurs near 9.5 μm. The tail of this absorption might contribute in part to the observed absorption at 10.6 μm. While this band can be revealed by calorimetric methods with a tuneable CO_2 laser, it is very clearly revealed by spectral emittance as shown in Fig. 2.

Although the sensitivity is adequate to reveal absorption coefficients of 0.0001 cm^{-1}, a zero correction of uncertain origin is still present.

The results in Fig. 2 clearly show that most if not all of the surface absorption band near 9.5 μm can be completely or largely eliminated by pumping in vacuum at an elevated temperature. In principle, it should be possible to deposit a protective coating over the sample once the surface absorbing layer has been removed. However, it may not be possible to form a layer offering sufficient protection to prevent regeneration of the surface absorbing layer, presumably occurring by surface oxidation.

The measurements were obtained in the following manner. In all cases, the sample temperature was 373K. The first measurement was for a chemically polished sample inserted in the instrument and pumped down. The second (middle curve of Fig. 2) was for a sample which was heated to about 250C for 60 hours in the emittance spectrometer and then brought down to 373K for measurement. The emittance spectrum of this sample shows a marked decrease in the intensity of the band at 9.5 μm. There still is a trace of this band in the spectrum. It is not clear at the present time whether this is associated with the sample or with some instrumental factor. It might be mentioned that in a separate experiment involving the emittance of a metal in this region, a trace of a band at 9.5 μm was present and might be due associated with the KBr window. Finally, the sample was exposed to the atmosphere for 24 hours and remeasured. The band at 9.5 μm then reappeared. While no studies of the rate of disappearance and reappearance of the band were made, these processes are not instantaneous and are of the order of several minutes. Both the baking time and exposure time to atmosphere are much greater than needed to show the effect. However, a time of the order of one hour is not enough for saturation.

4. SPECTRAL EMITTANCE OF BULK MATERIALS

The investigations of the temperature and frequency dependence of laser window materials is a long term objective of the program. The low temperature emittance spectra of pure KCl and NaF at low temperatures have been already reported by Stierwalt[1] and the intrinsic multiphonon absorption qualitatively behaves as expected. However, at low absorption coefficients, the temperature dependence was not as anticipated and may have been caused by deposition on material on a cold sample. These experiments were repeated and some deposition was definitely noted.

In addition, some samples were studied at temperatures above ambient where deposition would be unlikely to occur. Here the results again were in accord with expectations, but since it was not possible to go to temperatures above 250C, the change in absorption coefficient is not very large. Since the emittance depends both on the absorption coefficient and the sample temperature, uniform and accurate sample temperatures are necessary. It is believed this can be achieved when the thermal conductivity and sample geometry are such as to insure uniform sample temperature.

In conclusion, it is felt that these experiments will warrant repeating as they are quite important in order to make a good estimate of the absorption coefficient of low loss materials. Furthermore, improvements in the apparatus are equally essential as the low loss materials now available can not be accurately measured.

REFERENCES

1. Stierwalt, D.L.,Proc. Third Conference on High Power Infrared Laser Window Materials, Vol. I, p. 43, AFCRL-TR-0085.

2. Stierwalt, D.L. and Potter, R.F. (1967) Semiconductors and Semimetals, Vol. III, Chapter 3,(Academic Press).

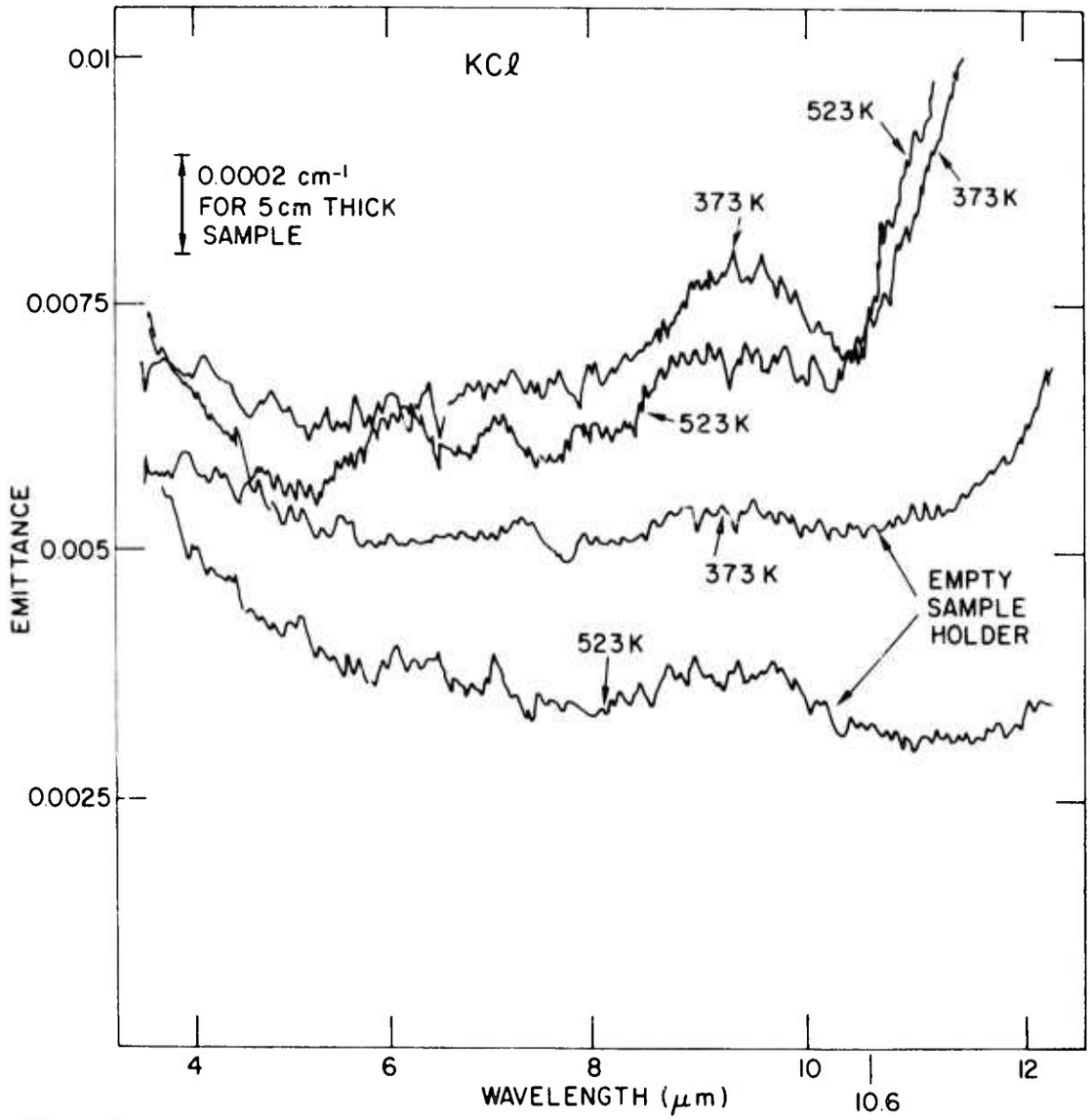

Fig. 1. Spectral emittance of KCl and empty sample holders at two different temperatures. No offset was used to separate the curves.

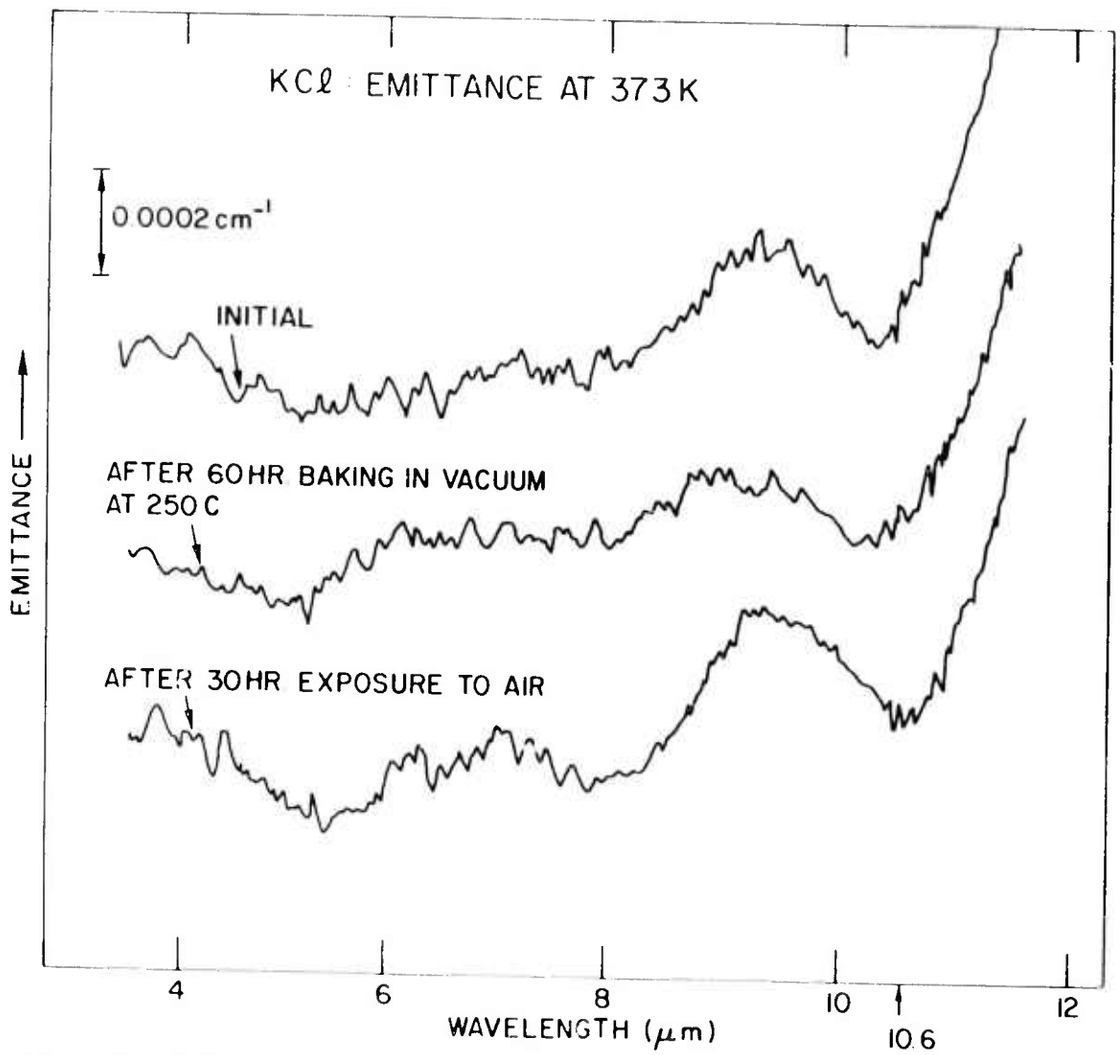

Fig. 2. Spectral emittance of KCl at 373K before and after heating in vacuum, as well as after re-exposure to air. The curves are offset for clarity and the corresponding absorption coefficient is shown. The zero level for absorption is probably determined by instrumental factors.

NEW INSTRUMENTATION

Donald L. Stierwalt
Naval Electronics Laboratory Center
San Diego, California 92152

To overcome the instrumental limitations and increase the sensitivity of the method, two approaches are being taken. The first is the construction of a new sample compartment for the present apparatus. The cryo-deposits on the sample surfaces mentioned earlier are obviously due to poor vacuum conditions. To obtain higher vacuum, the interior surfaces of the new sample compartment are chemically etched and black anodized instead of being painted black to achieve low reflectance. The "O" ring seals are replaced by indium gaskets, and a long one-inch tube to the ion pump has been replaced by a short two-inch line. These modifications should greatly improve the vacuum. In addition, the mirror and window surfaces are being cleaned and repolished to reduce the amount of energy from the sample holder which is scattered into the optical path. Redesigning the sample holders to have less radiating surface area should also reduce the scattered energy.

The second approach is the design and construction of a spectral emittance apparatus operating at cryogenic temperature. By maintaining the instrument at liquid nitrogen temperature, blackbody radiation from the components of the instrument is reduced to a very low level. Thus, variations in this radiation do not

produce a fluctuating zero level, as is the case with the room temperature instrument. With this source of noise eliminated, we can take advantage of the greater sensitivity of a cooled photoconductive detector operating under low photon flux conditions. The copper doped germanium detector we have obtained for use in this instrument has a D* of 1.05×10^{10} at high photon flux background. When used in an instrument which is operated at 77K, and with the background flux further limited by a short wavelength pass filter at 5K, the D* becomes 8×10^{12} at 10.6 microns. For the geometry used in the design of this instrument, this leads to the predicted noise equivalent emittance shown in the following table, assuming a 0.1 Hz bandwith:

λ (μ)	NEE
14.5	2.2×10^{-8}
10.6	2.6×10^{-8}
5.0	3.6×10^{-7}
3.8	4.5×10^{-6}
3.0	5.1×10^{-5}

SEPARATION OF SURFACE AND BULK ABSORPTION IN LASER CALORIMETRY

Julius Babiskin and Marvin Hass
U.S. Naval Research Laboratory
Washington, D.C. 20375

This following work has been supported entirely on internal NRL funds. However, the connection with ARPA supported laser window program is sufficiently close that it is reported here as it may be of value to other investigators in the field.

One of the major problems in dealing with infrared absorption in laser windows has been the separation of the absorption into a surface part and a bulk part. The usual way of doing this is by plotting the power absorbed as a function of length. The slope of such a curve is defined as the bulk absorption and the zero length intercept is defined as the absorption associated with the surfaces. A separation of surface and bulk absorption carried out in this manner implicitly assumes that all of the absorption can be separated into bulk and surface portions. In particular, it is assumed in a laser calorimetric experiment that scattering of the incident beam by the surface or bulk does not introduce any additional thermal heating of the sample. This assumption may be justified in many cases. However, at extremely low absorbing levels, the various contributions causing a thermal rise in the sample on laser irradiation are not clearly identifiable.

The purpose of the investigation to be described has been to try to effect a separation between the surface and bulk parts of absorption. The technique employed is the study of the time dependence of the thermal heating curve.

In samples of low thermal conductivity, the time dependence of the heating curve will be different for surface and bulk absorption. In samples of relatively high thermal conductivity (which includes most candidate laser window materials), this difference in the time dependence will be much less marked and has not yet been carried out and may be attempted in the future.

The experimental technique employed is essentially the same as that used for window studies in laser calorimetry and the apparatus is shown in Fig. 1. Here the sample is in the shape of a long cylindrical rod and this geometry greatly simplifies the calculations for low conductivity materials.[1] The samples employed are vitreous silica and the source is a He:Ne laser operating at 632.8 nm at 30 mw power. This particular choice of a low conductivity sample at a visible wavelength is particularly advantageous as it can accomplish the following: (1) Easy separation of surface and bulk effects and (2) Easy visual observation of scattered light.

In preliminary experiments, it was noted that the method of thermocouple attachment was particularly critical. In the visible this can be more important due to higher scattering. In the infrared no special difficulties with thermocouple attachment have been reported other than assuring good thermal contact to the sample. However, this might actually be an unrecognized problem. In particularly, employment of the usual method of cementing the thermocouple to the sample showed visual indication of light scattering at the point of attachment. For this reason, a new method involving deposition of a small metal mirror spot at the midpoint of the rod followed by cementing the thermocouple to this spot was found to produce the best results. Visual inspection revealed that light was reflected rather than scattered from a good metal mirror.

The results obtained can be illustrated schematically with reference to Fig. 2. In Fig. 2(a) a typical temperature-time curve in a laser calorimetry experiment is shown for bulk absorption only. On irradiation with a laser beam, the sample temperature will increase with a linear initial slope. In Fig. 2(c) the case for surface only absorption is shown. Since the absorbing region is several cm away from the thermocouple, there will be a short time delay before the temperature starts to increase. In Fig. 2(b) and 2(d), an initial jump at the laser turn-on and turnoff times is added and this can occur by absorption of scattered light at the point of thermocouple attachment.

The experimental results are shown in Fig. 3. The top section of Fig. 3 shows a calorimetric curve in which the absorption is sufficiently low that it is difficult to measure. It appears to be in the range of 10^{-5} cm^{-1} or less which is expected at 632.8 nm for a water-free fused silica. On the bottom section of Fig. 3 is shown the curve for the same sample, but without an aperture immediately in front of sample. After a short time delay, it appears that the sample temperature increases and this is to be expected of dominant surface absorption. Furthermore, when the beam is turned off, the sample temperature does not decrease exponentially as is expected for bulk only absorption. Not shown is a case of an irradiated glass which has bulk only absorption. The observed case is essentially the same as that for Fig. 2(a).

By inspection of Fig. 3, it can be deduced that there is some difference in the surface absorption between the top and bottom curves. However, the bulk absorption appears to be about the same, but could not be measured accurately at the power of about 30 mw. Since the only difference was inclusion of an aperture to act as a light baffle, it is not completely clear what is occurring.

Visual inspection of the sample in the two situations reveals that some light might be absorbed on the periphery of the cylindrical sample when the aperture is not employed.

These results are of significance in that this is the first reported technique capable of separating surface and bulk absorption in a single measurement. In principle, it should be applicable to laser window materials in the infrared as well and might result in the measurement of much lower absorption coefficients. Further, techniques such as those described would have to be employed for the study of uv and visible laser windows.

REFERENCES

1. White, K.I., and Midwinter, J.E. (1973) Opto-Electronics 5, 323.

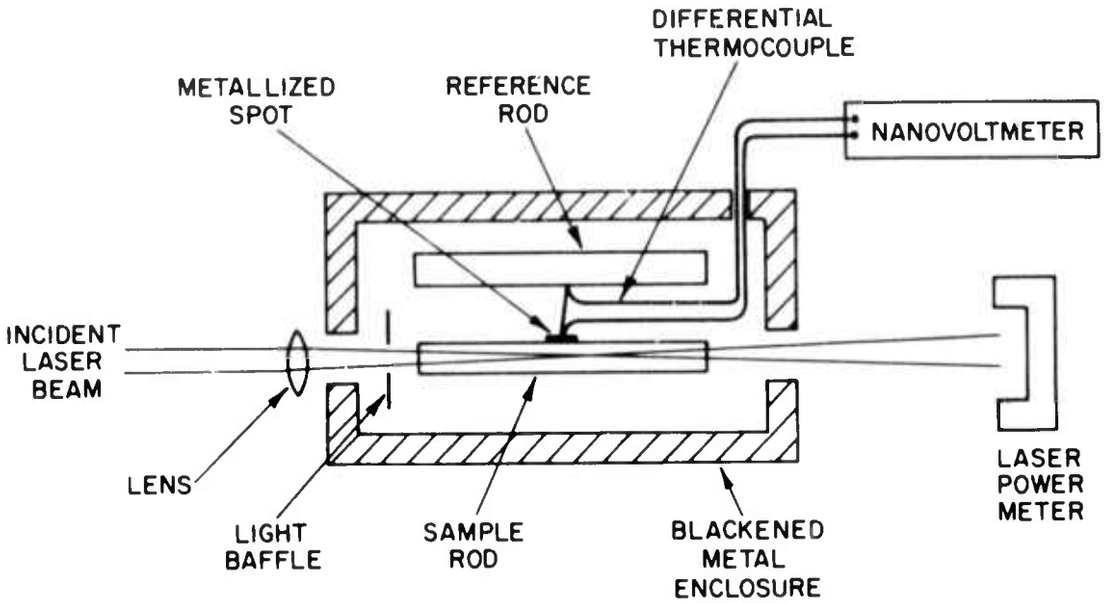

Fig. 1. Experimental arrangement for laser calorimetry of silica rods.

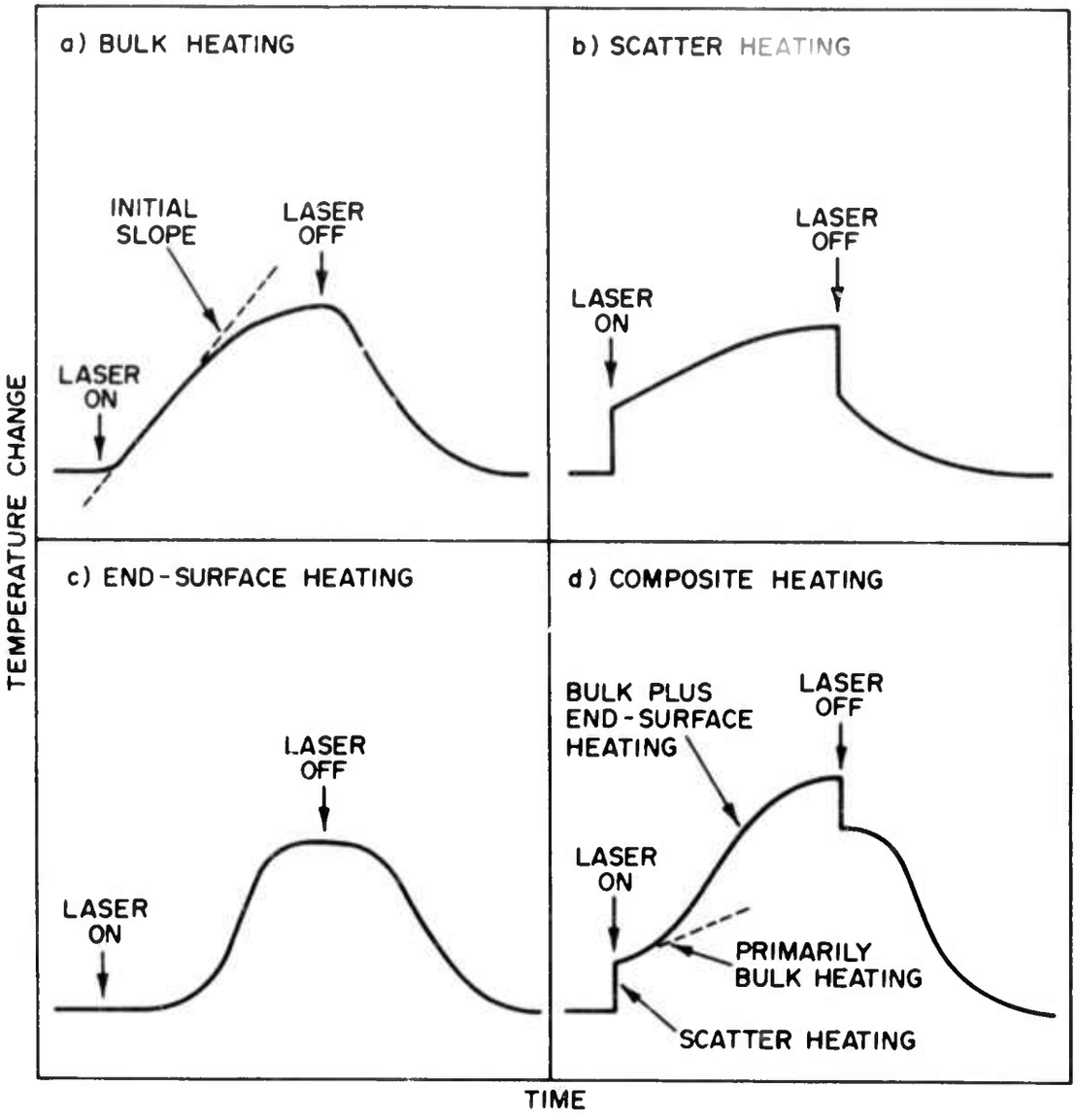

Fig. 2. Schematic illustrations of temperature-time curves for laser calorimetry in the following cases:

(a) bulk only absorption
(b) absorption of directed scattered light at thermocouple
(c) end surface only absorption
(d) composite absorption (both bulk and surface).

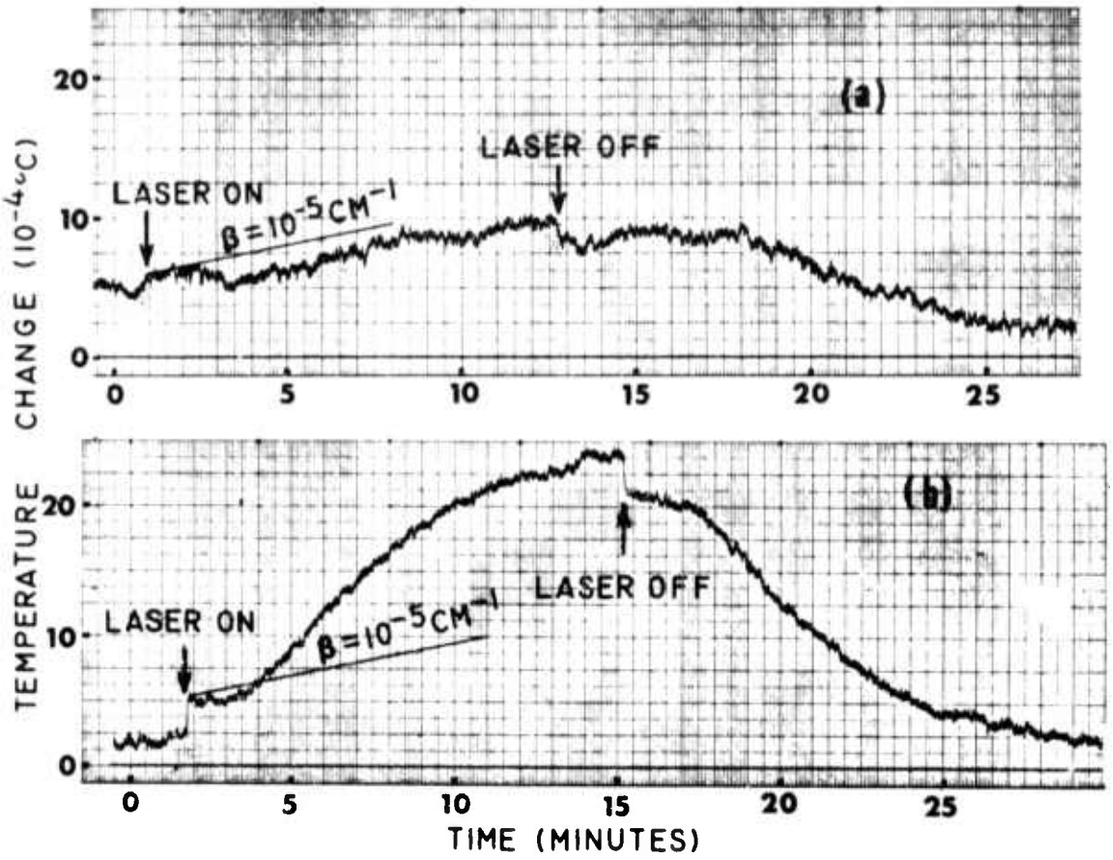

Fig. 3. (top) Temperature-time curve for a vitreous silica rod at 632.8 nm with aperture in front of sample.
(bottom) Temperature-time curve for a vitreous silica rod at 632.8 nm without aperture in front of sample.